

1-7-2023

Disruption of the Interaction Between Mutationally Activated G α Q and G $\beta\gamma$ Attenuates Aberrant Signaling

Jenna L Aumiller

Philip B Wedegaertner

Follow this and additional works at: <https://jdc.jefferson.edu/bmpfp>

 Part of the [Medical Biochemistry Commons](#), and the [Medical Molecular Biology Commons](#)

[Let us know how access to this document benefits you](#)

This Article is brought to you for free and open access by the Jefferson Digital Commons. The Jefferson Digital Commons is a service of Thomas Jefferson University's [Center for Teaching and Learning \(CTL\)](#). The Commons is a showcase for Jefferson books and journals, peer-reviewed scholarly publications, unique historical collections from the University archives, and teaching tools. The Jefferson Digital Commons allows researchers and interested readers anywhere in the world to learn about and keep up to date with Jefferson scholarship. This article has been accepted for inclusion in Department of Biochemistry and Molecular Biology Faculty Papers by an authorized administrator of the Jefferson Digital Commons. For more information, please contact: JeffersonDigitalCommons@jefferson.edu.

Disruption of the interaction between mutationally activated $G\alpha_q$ and $G\beta\gamma$ attenuates aberrant signaling

Received for publication, August 1, 2022, and in revised form, December 14, 2022. Published, Papers in Press, January 7, 2023.
<https://doi.org/10.1016/j.jbc.2023.102880>

Jenna L. Aumiller and Philip B. Wedegaertner*

From the Department of Biochemistry and Molecular Biology, Sidney Kimmel Medical College, Thomas Jefferson University, Philadelphia, Pennsylvania, USA

Edited by Kirill Martemyanov

Heterotrimeric G protein stimulation *via* G protein-coupled receptors promotes downstream proliferative signaling. Mutations can occur in $G\alpha$ proteins which prevent GTP hydrolysis; this allows the G proteins to signal independently of G protein-coupled receptors and can result in various cancers, such as uveal melanoma (UM). Most UM cases harbor Q209L, Q209P, or R183C mutations in $G\alpha_{q/11}$ proteins, rendering the proteins constitutively active (CA). Although it is generally thought that active, GTP-bound $G\alpha$ subunits are dissociated from and signal independently of $G\beta\gamma$, accumulating evidence indicates that some CA $G\alpha$ mutants, such as $G\alpha_{q/11}$, retain binding to $G\beta\gamma$, and this interaction is necessary for signaling. Here, we demonstrate that disrupting the interaction between $G\beta\gamma$ and $G\alpha_q$ is sufficient to inhibit aberrant signaling driven by CA $G\alpha_q$. Introduction of the I25A point mutation in the N-terminal α helical domain of CA $G\alpha_q$ to inhibit $G\beta\gamma$ binding, overexpression of the G protein $G\alpha_o$ to sequester $G\beta\gamma$, and siRNA depletion of $G\beta$ subunits inhibited or abolished CA $G\alpha_q$ signaling to the MAPK and YAP pathways. Moreover, in HEK 293 cells and in UM cell lines, we show that $G\alpha_q$ -Q209P and $G\alpha_q$ -R183C are more sensitive to the loss of $G\beta\gamma$ interaction than $G\alpha_q$ -Q209L. Our study challenges the idea that CA $G\alpha_{q/11}$ signals independently of $G\beta\gamma$ and demonstrates differential sensitivity between the $G\alpha_q$ -Q209L, $G\alpha_q$ -Q209P, and $G\alpha_q$ -R183C mutants.

Heterotrimeric G proteins ($G\alpha\beta\gamma$) are canonically activated through G protein-coupled receptors (GPCRs), which allows for GDP release from the $G\alpha$ subunit and further GTP binding. It is generally accepted that GTP binding on the $G\alpha$ subunit promotes an active conformation and allows for the dissociation from $G\beta\gamma$. Active GTP-bound $G\alpha$ proteins can further bind and stimulate downstream effectors (1, 2). Hydrolysis of GTP on the $G\alpha$ subunit promotes reassociation of the inactive $G\alpha\beta\gamma$ heterotrimer and completes the cycle. Several conserved amino acids, found in all $G\alpha$ subunits, are critical for the intrinsic GTP hydrolysis activity, and mutations of these residues prevent GTP hydrolysis and “lock” the $G\alpha$ protein in a constitutively active (CA), GTP-bound state (3, 4). Aberrant

CA mutations in $G\alpha$ proteins have been identified in various human tumors and diseases. For example, $G\alpha_s$ CA mutations have been identified in a subset of pancreatic tumors (5, 6). Mutations in $G\alpha_q$ and $G\alpha_{11}$ have also been described at residues Q209 and R183 in the majority of patients with uveal melanoma (UM). Q209L or Q209P mutations in $G\alpha_q$ or $G\alpha_{11}$ occur in 90% of UM patients, and mutations at R183 occur in about 5% of patients (7–10). Approximately, 50% of patients with UM develop distant metastatic disease to the liver; there are currently no effective therapies for metastatic UM. Upon metastatic diagnosis, the average survival is only 2 to 8 months, indicating the urgent importance of effective therapies for metastatic UM (11, 12).

The constitutive activity of $G\alpha_{q/11}$ in UM, driven by the activating Q209L/P and R183 mutations, promotes the stimulation of two major signaling pathways: 1) the mitogen-activated protein kinase (MAPK) pathway and 2) the Yes-associated protein and Transcriptional coactivator with PDZ-binding motif (YAP/TAZ) pathway. The MAPK cascade is stimulated by the direct binding of CA $G\alpha_{q/11}$ to phospholipase C- β (PLC- β), which hydrolyzes phosphatidylinositol 4,5-bisphosphate into diacylglycerol and inositol 1,4,5-trisphosphate. Diacylglycerol further activates PKC, which phosphorylates and activates RasGRP3. The further activation of Ras promotes the stimulation of the MAPK cascade and results in the phosphorylation and activation of ERK. Phospho-ERK (pERK) dimerizes and translocates into the nucleus to bind transcription factors and promote the transcription of proliferative genes (13). Mutationally active $G\alpha_{q/11}$ also stimulates the YAP/TAZ pathway through direct binding and activation of the RhoGEF Trio. In an inactive state, YAP is phosphorylated and remains cytoplasmic through mediators of the Hippo pathway. Activation of Trio leads to the stimulation of focal adhesion kinase, which inhibits mediators of the Hippo pathway and ultimately leads to the dephosphorylation and nuclear translocation of YAP. YAP binds to the TEA domain (TEAD) transcription factor in the nucleus to promote the transcription of genes involved in proliferation and cell survival (14, 15). To date, inhibitors for downstream targets of CA $G\alpha_{q/11}$ have been proven to be generally unsuccessful in disrupting the progression of metastatic UM (16–18).

Because $G\alpha_{q/11}$ stimulates multiple pathways, directly targeting CA $G\alpha_{q/11}$ may be a more promising therapeutic

* For correspondence: Philip B. Wedegaertner, philip.wedegaertner@jefferson.edu.

Gβγ binding is required for mutant Gα_q signaling

strategy for metastatic UM patients. There are currently no FDA-approved drugs that target Gα_{q/11}; however, the compounds YM-254890 (YM) and FR900359 (FR) have been shown to inhibit both WT and CA Gα_{q/11} and have shown promising results in cancer cell models (19–21). YM and FR have similar structures and are thought to prevent the release of GDP from Gα_{q/11} and ultimately inhibit GDP to GTP exchange (21–23). However, both YM and FR to date have had varying effects on UM tumor arrest and regression in pre-clinical UM mouse models (24, 25). Therefore, understanding how CA Gα_{q/11} is regulated in cells and further exploring other methods of inhibiting oncogenic Gα_{q/11} may provide therapeutic benefits for metastatic UM patients.

In an inactive, GDP-bound state, Gα proteins form heterotrimers with Gβγ. This interaction with Gβγ aids in plasma membrane localization to neighboring GPCRs and helps stabilize the complex for GTP exchange (26–31). Crystal structures indicate that the inactive, GDP-bound Gα subunit has two main points of contact with Gβγ: 1) a central switch region, which undergoes a conformational change upon GTP binding and 2) an N-terminal α helical domain (32–34). It is generally accepted in the field that during nucleotide exchange, the Gα subunit can dissociate from the Gβγ subunit; therefore, it would be reasonable to assume that the CA Gα_{q/11} mutants commonly found in UM would have minimal interaction with the Gβγ. However, work in our lab and others suggest that the CA Gα_q-Q209L mutant retains a functionally important interaction with Gβγ *via* the N-terminal α helical domain (32–34). Previous work in our lab indicates that a single point mutation (I25A) in the N-terminal α helix of WT Gα_q is sufficient to disrupt binding to Gβγ, and this disruption of binding further prevents GPCR-dependent signaling of WT Gα_q (35). The I25A N-terminal Gβγ-binding mutation was also sufficient to disrupt overactive inositol phosphate (IP) production for the CA Gα_q-R183C mutant. Understanding the role of Gβγ in the oncogenic signaling activity of CA Gα_q could address the gaps in knowledge of the cellular regulation of CA Gα_q and further offer Gβγ as a potential target for disrupting aberrant signaling in UM.

Here, we tested the hypothesis that disrupting the interaction between Gβγ and the CA Gα_q mutants commonly found in UM patients—Q209L (QL), Q209P (QP), and R183C (RC)—is sufficient to inhibit oncogenic signaling of these mutationally active Gα_q. We provide evidence that disrupting the interaction between CA Gα_q and Gβγ significantly inhibits Gα_q-mediated activation of the MAPK and YAP/TAZ pathways. Surprisingly, we show differential sensitivity between Gα_q-QL and the Gα_q-QP/RC mutants in that oncogenic signaling by Gα_q-QP and Gα_q-RC is more sensitive to the disruption of Gβγ binding than Gα_q-QL.

Results

N-terminal Gβγ-binding mutation I25A inhibits oncogenic signaling by CA Gα_q mutants

Previous work has shown that the activation of downstream effectors of Gα_q, such as PLC-β, requires the binding of Gα_q to

Gβγ (35). Furthermore, recent studies have indicated that CA Gα_q-Q209L proteins retain binding to Gβγ at the N-terminal α-helical region (36). It has been established that the I25A point mutation within the N-terminal α-helical domain of Gα_q is sufficient to disrupt the interaction between Gα_q and Gβγ and consequently inhibit the GPCR-dependent signaling of WT Gα_q (35). Thus, we hypothesized that introducing the I25A mutation to disrupt binding to Gβγ would inhibit oncogenic signaling through the CA Gα_q-Q209L (QL), Q209P (QP), and R183C (RC) mutants. To monitor the activity of the YAP/TAZ pathway, we transfected the CA mutants, with and without the I25A mutation, into HEK 293 Gα_{q/11} CRISPR-Cas9 KO cells and monitored YAP activity using the TEAD luciferase reporter assay, which is stimulated in response to YAP activation and nuclear translocation. Gα_q-QL, Gα_q-QP, and Gα_q-RC all showed strong activation in the assay. Cells expressing the pcDNA3 vector and WT Gα_q were used as negative controls and indicated no significant change in TEAD luciferase reporter activity (Fig. 1A). The Gα_q-QL-C9,10S palmitoylation-deficient mutant was used as a negative control for Gα_q-QL. The C9,10S mutation in WT Gα_q has been previously established to prevent plasma membrane localization and consequently prevent GPCR-dependent activation (37); likewise, we now show that Gα_q-QL-C9,10S is unable to stimulate TEAD-dependent luciferase activity. Interestingly, Gα_q-I25A-QL displayed a decreased ability compared to Gα_q-QL to activate TEAD luciferase activity, yet retained significantly higher activity than the Gα_q-QL-C9,10S control. In contrast, the introduction of the I25A mutation abolished the ability of Gα_q-QP and Gα_q-RC to stimulate TEAD luciferase. These data demonstrate that the introduction of the I25A mutation inhibits oncogenic signaling to the YAP pathway by the CA Gα_q-QL/P and Gα_q-RC mutants. These results also suggest potential differential sensitivity between the CA Gα_q-QL and Gα_q-QP/RC mutants.

To further monitor YAP activity and the differential sensitivity between the CA Gα_q-I25A mutants, we used immunofluorescence microscopy to examine the cellular localization of YAP (Fig. 1B). It has been previously established that activation of the Rho-dependent YAP pathway results in stabilization and dephosphorylation of YAP and its subsequent translocation into the nucleus (38, 39). The YAP pathway was not stimulated in cells expressing the pcDNA3 vector and WT Gα_q, as shown by the low expression and cytoplasmic localization of YAP. Expression of Gα_q-QL indicated strong nuclear localization of YAP, and treatment with the Gα_{q/11} inhibitor YM-254890 (YM) as a control resulted in the loss of nuclear YAP and its accumulation in the cytoplasm. Gα_q-I25A-QL also promoted nuclear localization of YAP, consistent with its retention of signaling in the TEAD-luciferase assay (Fig. 1A). Cells expressing CA Gα_q-QP and Gα_q-RC had robust nuclear YAP localization, indicating stimulation of this pathway. However, Gα_q-I25A-QP and Gα_q-I25A-RC failed to stimulate the nuclear localization of YAP, as indicated by the cytoplasmic localization of YAP. Similar to the TEAD-luciferase reporter assay results, this data suggests that Gα_q-I25A-QL is more resistant to

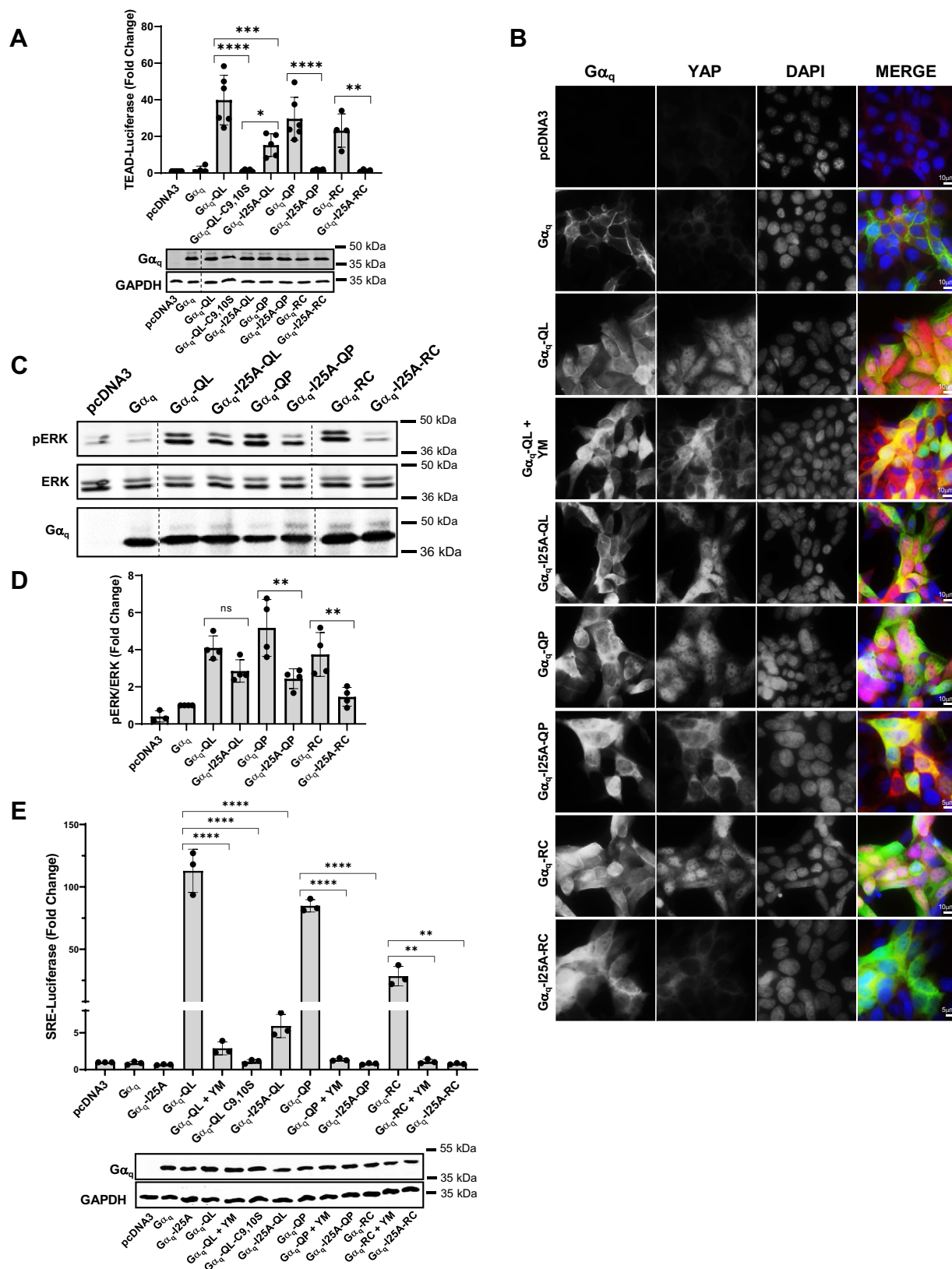


Figure 1. Oncogenic signaling by constitutively active Ga_q is inhibited by I25A N-terminal Gβγ-binding mutation. A, HEK 293 Ga_q/11 KO cells were transfected with pcDNA3, WT Ga_q, Ga_q-QL, Ga_q-QL-C9,10S, Ga_q-I25A-QL, Ga_q-QP, Ga_q-I25A-QP, Ga_q-RC, or Ga_q-I25A-RC, along with 8x-GT1C Luciferase and Renilla control plasmids. Cell lysates were prepared, and luciferase assays were performed and quantified. Graph indicates fold change over pcDNA3. Results are shown as mean ± SD. Statistical significance is indicated (n = 6 for Ga_q-QL, Ga_q-QP; n = 5 for pcDNA3, Ga_q-QL-C9,10S, Ga_q-I25A-QL; n = 4 for WT Ga_q, Ga_q-I25A-QP, Ga_q-RC, Ga_q-I25A-RC. *p < 0.05; **p < 0.01; ***p < 0.005; ****p < 0.0001, two-way ANOVA, Sidák's multiple comparison's test). Lysates were also immunoblotted to detect relative expression levels of the various Ga_q mutants along with GAPDH controls, and a representative immunoblot is shown.

Gβγ binding is required for mutant Gα_q signaling

disruption of signaling than the Gα_q-I25A-QP and Gα_q-I25A-RC mutants. In immunofluorescence microscopy studies, we also examined the subcellular localization of the CA Gα_q mutants with and without the I25A mutation (Fig. S1). Previous work has demonstrated that the interaction with Gβγ is crucial for palmitoylation and further membrane localization of Gα_q (27). Gα_q-QL and Gα_q-RC were localized to the plasma membrane in transfected cells. The introduction of the I25A mutation does not significantly impact the plasma membrane localization of Gα_q-QL but results in partial loss of plasma membrane localization of Gα_q-RC (Fig. S1). Interestingly, Gα_q-QP had only partial plasma membrane association, and introduction of the I25A mutation resulted in an almost complete loss of plasma membrane localization (Fig. S1). Thus, decreased plasma membrane localization of Gα_q-RC and Gα_q-QP when interaction with Gβγ is disrupted through introduction of the I25A mutation provides at least a partial mechanistic explanation for their loss of signaling. These differences in cellular localization of the Gα_q-I25A-QL, Gα_q-I25A-QP, and Gα_q-I25A-RC (Fig. S1) likely contribute to the differential sensitivity in aberrant cell signaling (Fig. 1).

Along with stimulation of the YAP pathway, CA Gα_{q/11} also canonically stimulates PLC-β and further activates the MAPK cascade. To monitor the effects of the I25A mutants on the MAPK pathway, we quantified pERK levels in HEK 293 Gα_{q/11} KO cells transfected with the CA Gα_q constructs and the I25A mutants (Fig. 1, C and D). Expression of CA Gα_q-QL resulted in pERK stimulation >4-fold compared to cells transfected with pcDNA3 or WT Gα_q. The Gα_q-I25A-QL mutant also activated pERK at a slightly decreased level compared to Gα_q-QL, although the difference was not statistically significant. Interestingly, the Gα_q-QP and Gα_q-RC mutants stimulated pERK, but pERK activity was significantly decreased in cells expressing the Gα_q-I25A-QP and Gα_q-I25A-RC mutants (Fig. 1, C and D). The effects of the I25A mutants on MAPK activity were further validated with the serum response element (SRE) luciferase reporter assay, which monitors both Rho and MAPK-dependent activity (Fig. 1E). As indicated, the CA Gα_q-QL mutant robustly stimulated SRE-dependent luciferase activity. Introduction of the I25A mutation into Gα_q-QL (Gα_q-I25A-QL) strongly inhibited the ability to stimulate SRE luciferase activity, similar to the lack of signaling by the Gα_q-QL-C9,10S palmitoylation-deficient mutant and the loss of signaling upon treatment of cells expressing Gα_q-QL with YM. As expected, the CA Gα_q-QP and Gα_q-RC mutants also robustly stimulated SRE luciferase activity, while the Gα_q-I25A-QP and Gα_q-I25A-RC mutants completely failed to stimulate luciferase activity, similar to cells treated

with YM (Fig. 1E). The decreased signaling by Gα_q-I25A-QL in comparison to Gα_q-QL is much more drastic in the SRE luciferase assay than the pERK immunoblot assay (Fig. 1, C and D). Although this is somewhat surprising since the SRE luciferase readout is downstream of the MAPK pathway, we note that the SRE luciferase assay provides a very high signal-to-noise readout for Gα_q-QL signaling (>100-fold above basal vector alone or WT Gα_q) and is consistently very sensitive to disruption of Gα_q-QL signaling (e.g., Gα_q-I25A-QL only signals 5–6-fold above basal). Taken together, these results indicate that the introduction of the I25A mutation to disrupt binding to Gβγ inhibited oncogenic signaling of the CA Gα_q mutants through the YAP and MAPK pathways, and the Gα_q-QP and Gα_q-RC mutants are more sensitive to the I25A mutation than Gα_q-QL.

Differential association with Gβγ by CA Gα_q and Gα_q-I25A mutants

Previous studies in our lab have elucidated that CA Gα_q-QL has an increased association with Gβγ compared to Gα_q-RC (35). Furthermore, we have also shown that Gα_q-I25A-QL maintains a substantial association with Gβγ compared to an almost complete loss of Gβγ association when the I25A mutation is introduced into WT Gα_q or Gα_q-RC (35). It has also been previously established that Gα_q-QP has reduced binding to effector proteins, such as p63RhoGEF, Trio, and GRK2 (40). Thus, we wanted to further characterize the interactions between Gβγ and CA Gα_q-QL/P and Gα_q-RC and the corresponding I25A mutants. To study this, we transiently transfected the WT or CA Gα_q and I25A mutants into HEK293 cells which stably expressed 6x-His-Gβ_{1γ2} and pulled down Gβ₁ using Ni-NTA beads. The relative association of Gα_q bound to Gβ_{1γ2} was revealed through immunoblotting (Fig. 2A) and was further quantified (Fig. 2B). As expected, WT Gα_q displayed a strong pull down with Gβ_{1γ2}, but the introduction of the I25A mutation into WT Gα_q strongly decreased this interaction, indicating that the I25A mutation disrupts binding between Gα_q and Gβγ. Interestingly, Gα_q-QL had a similar binding association to Gβ_{1γ2} with that of WT Gα_q, and Gα_q-QL bound significantly stronger to Gβ_{1γ2} than Gα_q-QP and Gα_q-RC (Fig. 2, A and B). Furthermore, Gα_q-I25A-QL was more strongly bound to Gβ_{1γ2} than Gα_q-I25A-QP and Gα_q-I25A-RC (Fig. 2, A and B). We did not see a statistically significant difference in association with Gβγ between Gα_q-QP and Gα_q-RC and their corresponding I25A mutants. This is likely due to the low initial binding to Gβγ with both Gα_q-QP and Gα_q-RC. Although we previously demonstrated the

B, HEK 293 Gα_{q/11} KO cells transfected with pcDNA3, WT Gα_q, Gα_q-QL, Gα_q-I25A-QL, Gα_q-QP, Gα_q-I25A-QP, Gα_q-RC, or Gα_q-I25A-RC. Gα_q-QL + YM indicates that cells were transfected with Gα_q-QL and treated with 1 μM YM for 16 h. Coverslips were processed for immunofluorescence microscopy to detect Gα_q, YAP, and nuclei (DAPI) (n = 4) as described under [Experimental procedures](#), and representative images are shown. C and D, HEK 293 Gα_{q/11} KO cells were transfected with pcDNA3, WT Gα_q, Gα_q-QL, Gα_q-I25A-QL, Gα_q-QP, Gα_q-I25A-QP, Gα_q-RC, or Gα_q-I25A-RC. C, cell lysates were prepared and immunoblotted for pERK, ERK, and Gα_q. D, pERK/ERK signal intensities were quantified. Graph indicates fold change of pERK/ERK levels over WT Gα_q. Results are shown as mean ± SD. Statistical significance is indicated. (n = 4; n = 3 for pcDNA3, **p < 0.01, two-way ANOVA, Sidák's multiple comparison's test). E, HEK 293 Gα_{q/11} KO cells were transfected with pcDNA3, WT Gα_q, Gα_q-I25A, Gα_q-QL, Gα_q-I25A-QL, Gα_q-QP, Gα_q-I25A-QP, Gα_q-RC, or Gα_q-I25A-RC, along with SRE Luciferase and Renilla control plasmids. Gα_q-QL, Gα_q-QP, and Gα_q-RC conditions were treated with 1 μM YM for 16 h as indicated. Lysates were immunoblotted to detect Gα_q and GAPDH protein levels. Cell lysates were prepared and luciferase assays were performed and quantified. Results are shown as mean ± SD. Graph indicates fold change over pcDNA3. Statistical significance is indicated. (n = 3; **p < 0.01; ****p < 0.0001, two-way ANOVA, Sidák's multiple comparison's test). pERK, phospho-ERK; YAP, Yes-associated protein.

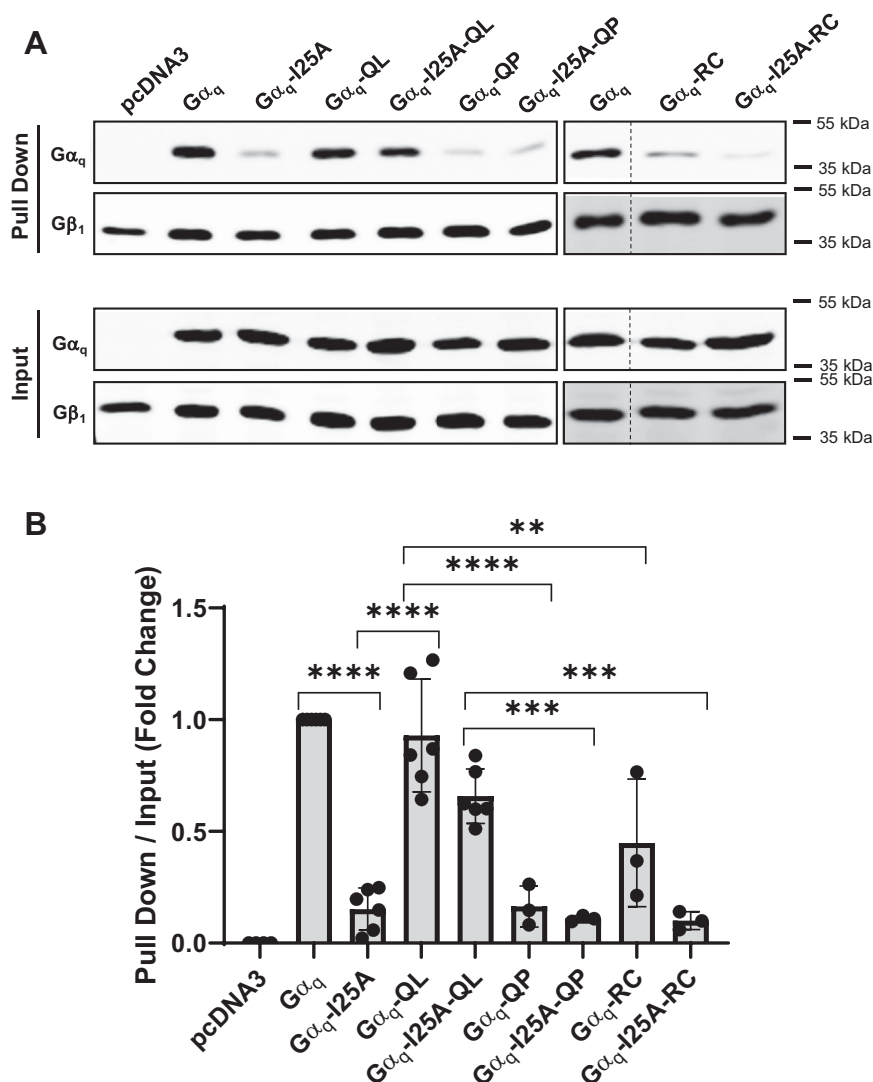


Figure 2. Constitutively active Gα_q and Gα_q-I25A mutants have differential association with Gβγ. A and B, HEK 293 6x-His-β₁Y₂ stable cells were transfected with pcDNA3, WT Gα_q, Gα_q-I25A, Gα_q-QL, Gα_q-I25A-QL, Gα_q-QP, Gα_q-I25A-QP, Gα_q-RC, or Gα_q-I25A-RC. The cells were lysed, and an Ni-NTA pull-down assay was performed, as described under [Experimental procedures](#). A, pull down and input lysates were immunoblotted using antibodies for the proteins indicated. B, the Gα_q pull-down signal intensities were quantified and normalized to the respective Gα_q input signal intensity. Results are shown as mean ± SD. Statistical significance is indicated (n = 6 for pcDNA3, WT Gα_q, Gα_q-I25A, Gα_q-QL, Gα_q-I25A-QL; n = 3 for Gα_q-QP, Gα_q-I25A-QP, Gα_q-RC, or Gα_q-I25A-RC, **p < 0.01; ***p < 0.005; ****p < 0.0001, two-way ANOVA, Šidák's multiple comparison's test).

surprising ability of Gα_q-QL to interact strongly with Gβγ and the poor interaction of Gα_q-RC with Gβγ, we now show a dramatically decreased association of Gα_q-QP with Gβγ compared to Gα_q-QL, even though both have a mutation of Q209. This differential binding to Gβγ between the CA Gα_q mutants likely contributes to the varying sensitivity in oncogenic signal disruption between the I25A mutants (Fig. 1).

Expression of Gα_o to sequester endogenous Gβγ inhibits signaling by Gα_q-QL/P and Gα_q-RC

Considering that inhibiting the association between the CA Gα_q mutants and Gβγ with the N-terminal I25A mutation significantly inhibited oncogenic signaling, we wanted to explore other methods of disrupting the interaction between Gβγ and CA Gα_q. Overexpression of Gα_i family proteins has

been previously used to sequester endogenous Gβγ in cells (41–43). Thus, we overexpressed Gα_o, a Gα_i family member, with the CA Gα_q-QL/QP and Gα_q-RC mutants to bind and sequester endogenous Gβγ to ultimately decrease or prevent binding of endogenous Gβγ to the expressed Gα_q. We also used a Gα_o G2A mutant as a negative control. The G2A mutation prevents both myristoylation and palmitoylation; this renders Gα_o cytoplasmic and poorly able to bind Gβγ due to its inability to localize to cellular membranes (44). YAP activity was monitored using the TEAD luciferase reporter assay with cotransfection of the CA Gα_q mutants and increasing amounts of the Gα_o expression plasmids (Fig. 3A). Interestingly, cotransfection with 200 ng of the Gα_o DNA was required to decrease Gα_q-QL stimulation of TEAD luciferase activity by 63%. In comparison, cotransfection with 100 ng of Gα_o plasmid DNA achieved 83% and 84% reduction in signaling by

Gβγ binding is required for mutant Ga_q signaling

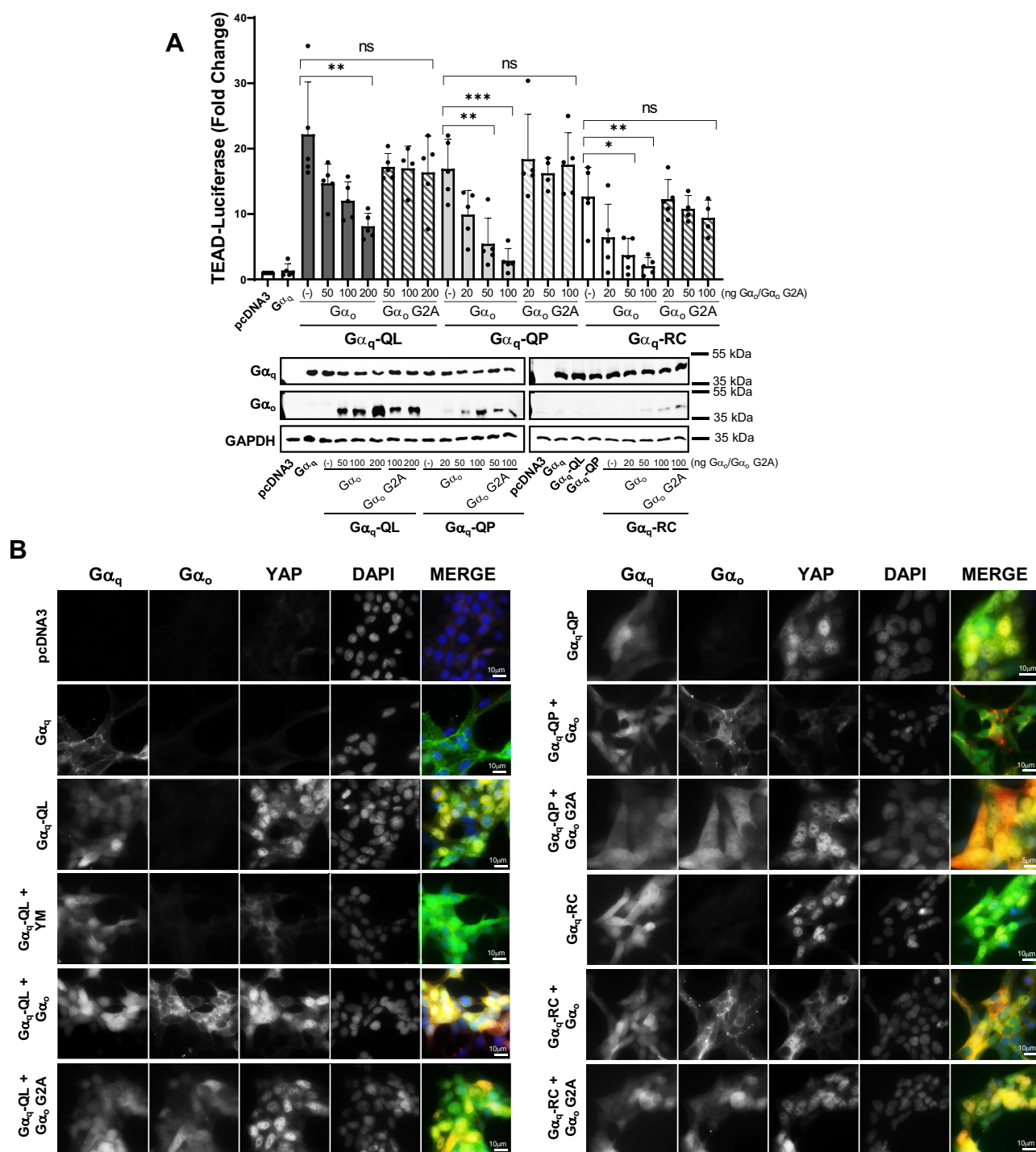


Figure 3. $G\alpha_o$ expression to bind $G\beta\gamma$ inhibits YAP signaling from constitutively active $G\alpha_q$ mutants. A, HEK 293 $G\alpha_{q/11}$ KO cells were transfected with pcDNA3, WT $G\alpha_q$, $G\alpha_q$ -QL, $G\alpha_q$ -QP, or $G\alpha_q$ -RC, along with 8x-GT1C Luciferase and Renilla control plasmids and along with varying amounts of $G\alpha_o$ or $G\alpha_o$ -G2A expression plasmids. Cell lysates were prepared and luciferase assays were performed and quantified. Graph indicates fold change over pcDNA3. Results are shown as mean \pm SD. Statistical significance is indicated (n = 4 or 5, * p < 0.05; ** p < 0.01; *** p < 0.005, two-way ANOVA, Sidák's multiple comparison's test). Lysates were immunoblotted for $G\alpha_q$, $G\alpha_o$, and GAPDH protein levels. B, HEK 293 $G\alpha_{q/11}$ KO cells were transfected with pcDNA3, WT YFP- $G\alpha_q$, YFP- $G\alpha_q$ -QL, YFP- $G\alpha_q$ -QP, or YFP- $G\alpha_q$ -RC, along with 250 ng of $G\alpha_o$ or $G\alpha_o$ G2A. Cells indicated with $G\alpha_q$ -QL + YM were transfected with YFP- $G\alpha_q$ -QL and treated with 1 μ M YM for 16 h. YFP- $G\alpha_q$, $G\alpha_o$, YAP, and nuclei (DAPI) stains were imaged via immunofluorescence microscopy (n = 3). YAP, Yes-associated protein.

$G\alpha_q$ -QP and $G\alpha_q$ -RC, respectively. Transfection with the control $G\alpha_o$ G2A constructs did not reduce the luciferase reporter activity in response to the CA $G\alpha_q$ mutants (Fig. 3A).

The ability of the expression of $G\alpha_o$ to reduce CA $G\alpha_q$ -stimulated YAP activity was also monitored through nuclear localization of YAP by immunofluorescence microscopy.

Gα_o localized strongly at cellular membranes, while the Gα_o G2A mutant was primarily cytoplasmic, indicating the expected localization of the proteins. Strong nuclear YAP was detected with the CA Gα_q-QL, Gα_q-QP, and Gα_q-RC mutants, indicating stimulation of the YAP pathway (Fig. 3B). As expected, expression of Gα_o G2A with the CA Gα_q mutants did not disrupt nuclear localization of YAP. Overexpression of Gα_o inhibited YAP nuclear localization stimulated by Gα_q-QP and Gα_q-RC (Fig. 3B). Conversely, cotransfection of Gα_o with Gα_q-QL failed to prevent strong YAP nuclear localization (Fig. 3B), further suggesting that the Gα_q-QP and Gα_q-RC mutants are more sensitive to Gβγ binding disruption than Gα_q-QL.

To monitor the effects of Gα_o expression and subsequent Gβγ sequestration on CA Gα_q-promoted MAPK activity, we immunoblotted for pERK levels (Fig. 4, A and B). The expression of the CA Gα_q mutants resulted in strong stimulation of pERK. Expression of Gα_o resulted in no significant decrease in pERK activity for Gα_q-QL. However, cotransfection of Gα_q-QP or Gα_q-RC with 50 ng and 100 ng of Gα_o plasmid resulted in a strong decrease in pERK activity (Fig. 4, A and B). There was no significant change in pERK levels with the Gα_o G2A control (Fig. 4, A and B). These results were further validated using the SRE luciferase reporter assay (Fig. 4C). Expression of Gα_q-QL, Gα_q-QP, and Gα_q-RC robustly activated SRE-dependent luciferase activity, while treatment with YM abolished luciferase activity. Consistent with results from the other signaling assays (Figs. 3 and 4, A and B), cotransfection with 50 ng Gα_o plasmid was sufficient to completely abolish Gα_q-QP- and Gα_q-RC-stimulated SRE luciferase activity, while up to 250 ng of Gα_o plasmid was required for near complete inhibition of Gα_q-QL-stimulated SRE luciferase activity (Fig. 4C). These findings indicate that the expression of Gα_o to sequester endogenous Gβγ inhibits the signaling activity of Gα_q-QL/P and Gα_q-RC. The results also further validate that the Gα_q-QL CA mutant is less sensitive to signaling disruption than the Gα_q-QP and Gα_q-RC mutants.

Gα_o expression inhibits the binding of Gβγ to CA Gα_q mutants

Next, we wanted to confirm that the expression of Gα_o could sequester Gβγ and inhibit the binding of Gβγ to Gα_q-QL/P and Gα_q-RC. To examine this, we coexpressed Gα_o or Gα_o G2A with the CA Gα_q mutants in 6x-His-Gβ₁γ₂ HEK 293 stable cells and pulled down Gβ₁γ₂ with Ni-NTA beads. Immunoblots were used to detect Gα_q and Gα_o bound to Gβ₁ (Fig. 5, A and B). As indicated in Figure 2, Gα_q-QL had a stronger binding association with Gβ₁ than Gα_q-QP and Gα_q-RC. Gα_o was bound to Gβ₁ in the pull-down extract, but Gα_o G2A had minimal to no interaction with Gβ₁ as expected. The expression of Gα_o resulted in significantly decreased binding of Gα_q-QL to Gβ₁ (Fig. 5, A and B). Expression of Gα_o consistently resulted in a noticeable decrease in the pull down of Gα_q-QP and Gα_q-RC with Gβγ, but this did not reach statistical significance due to the already low level of Gα_q-QP and Gα_q-RC association with Gβγ in the absence of Gα_o.

expression. These findings confirm that overexpression of Gα_o sequesters Gβγ and prevents binding of Gα_q-QL/P and Gα_q-RC to Gβγ.

Depletion of Gβ_{1/2} inhibits oncogenic signaling by Gα_q-Q209P in UM cell lines

Our studies demonstrate that disrupting the interaction between Gβγ and CA Gα_q through the N-terminal I25A mutation or expression of Gα_o is sufficient to inhibit overactive Gα_q signaling in HEK 293 Gα_{q/11} KO cells. We next wanted to determine if inhibiting Gβγ binding to CA Gα_q would be sufficient to disrupt oncogenic signaling in UM cells containing the Gα_q-QL or Gα_q-QP mutants. To study this, we depleted Gβ₁ and Gβ₂, two predominant Gβ subunits, through siRNA transfections. Sufficient knockdown of Gβ₁ and Gβ₂ was first validated in HEK 293 Gα_{q/11} KO cells (Fig. 6, A and B). siRNA molecules specific for Gβ₁, Gβ₂, and both Gβ₁ and Gβ₂ were transfected into the HEK 293 Gα_{q/11} KO cells, and WT Gα_q, Gα_q-QL, or Gα_q-QP constructs were transfected after 24 h. pERK levels were detected and quantified through immunoblotting (Fig. 6, A and B). The results indicate that siRNA depletion of Gβ_{1/2} significantly disrupted pERK activity driven by both Gα_q-QL and Gα_q-QP (Fig. 6, A and B). Gβ₁ or Gβ₂ siRNA knockdown alone was insufficient to significantly inhibit pERK activation (Fig. 6, A and B). Considering the effectiveness of Gβ_{1/2} depletion on pERK activity in the HEK 293 Gα_{q/11} KO cells, we decided to knock down Gβ_{1/2} in four UM cell lines: 1) Mel202 (Gα_q-Q209L mutation), 2) 92.1 (Gα_q-Q209L mutation), 3) OMM1.3 (Gα_q-Q209P mutation), and 4) UM001 (Gα_q-Q209P mutation). We also used the OCM-3 cell line as a control. The oncogenic activity of OCM-3 cells is driven by mutant BRAF (V600E) as opposed to mutant Gα_{q/11}; thus, we would expect Gβ_{1/2} depletion to have minimal effect on pERK activity (45). All cell lines were treated with control or Gβ_{1/2} siRNA for 96 h. Mel202, 92.1, OMM1.3, and UM001 cells were also treated with YM as a control. pERK levels were immunoblotted (Fig. 6C) and quantified (Fig. 6D). Interestingly, the OMM1.3 and UM001 cell lines which contain the Gα_q-Q209P mutation had significantly decreased pERK levels with Gβ_{1/2} knockdown, similar to that of YM treatment (Fig. 6, C and D). There was no significant difference in pERK levels with Gβ_{1/2} depletion in the Mel202 and 92.1 cells which contain the Gα_q-Q209L mutation (Fig. 6, C and D). This data further suggests that there is differential sensitivity to the inhibition of oncogenic signaling between cell lines with the Gα_q-Q209L and Gα_q-Q209P mutations.

Discussion

The results presented in this study demonstrate the importance of Gβγ for signaling by CA mutants of Gα_q and show a surprising differential sensitivity of CA Gα_q mutants to the inhibition of signaling upon disruption of their interaction with Gβγ. We used two methods to disrupt Gβγ interaction with CA Gα_q—introduction of a Gβγ-binding disrupting mutation, I25A, into CA Gα_q and sequestration of

Gβγ binding is required for mutant Gα_q signaling

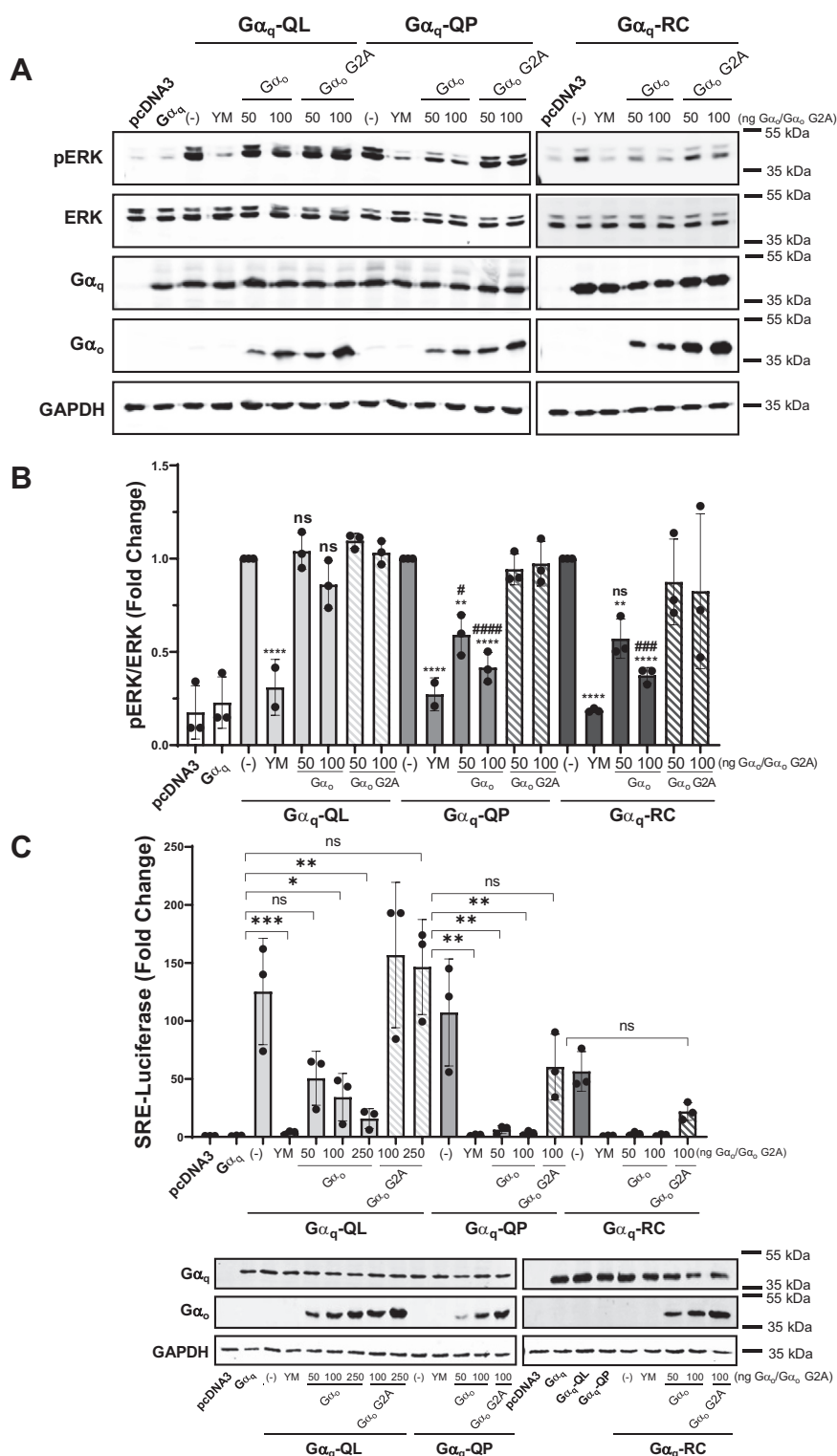


Figure 4. Constitutively active Gα_q-dependent MAPK signaling is inhibited by overexpression of Gα_o. A and B, HEK 293 Gα_{q/11} KO cells were transfected with pcDNA3, WT Gα_q, Gα_q-QL, Gα_q-QP, or Gα_q-RC, along with 50 ng or 100 ng of Gα_o or Gα_o-G2A. YM indicates expression of Gα_q-QL, Gα_q-QP, or Gα_q-RC with treatment with 1 μM YM for 16 h. A, cell lysates were prepared and immunoblotted for pERK, ERK, Gα_q, Gα_o, and GAPDH. B, pERK/ERK signal intensities were quantified. Graph indicates pERK/ERK signal intensities normalized to Gα_q-QL, Gα_q-QP, or Gα_q-RC without Gα_o expression. Results are shown as mean ± SD. Statistical significance is indicated. (* indicates significance between Gα_q-QL, Gα_q-QP, or Gα_q-RC and treatment with YM or Gα_o; # indicates significance between treatment with Gα_o and corresponding concentration of Gα_o G2A) (n = 3; n = 2 for Gα_q-QL and Gα_q-QP with YM treatment, *p < 0.05; **p < 0.01; ***p < 0.005; ****p < 0.0001, two-way ANOVA, Šidák's multiple comparison's test). C, HEK 293 Gα_{q/11} KO cells were transfected with pcDNA3, WT Gα_q, Gα_q-QL, Gα_q-QP, or Gα_q-RC, along with varying concentrations of Gα_o or Gα_o G2A. YM indicates expression of Gα_q-QL, Gα_q-QP, or Gα_q-RC with 1 μM treatment of YM for 16 h. Cell lysates were prepared and luciferase assays were performed and quantified. Results are shown as mean ± SD. Graph indicates fold change over pcDNA3. Statistical significance is indicated (n = 3; *p < 0.05; **p < 0.01; ***p < 0.005, two-way ANOVA, Šidák's multiple comparison's test). Lysates were immunoblotted for Gα_q, Gα_o, and GAPDH protein levels. MAPK, mitogen-activated protein kinase; pERK, phospho-ERK.

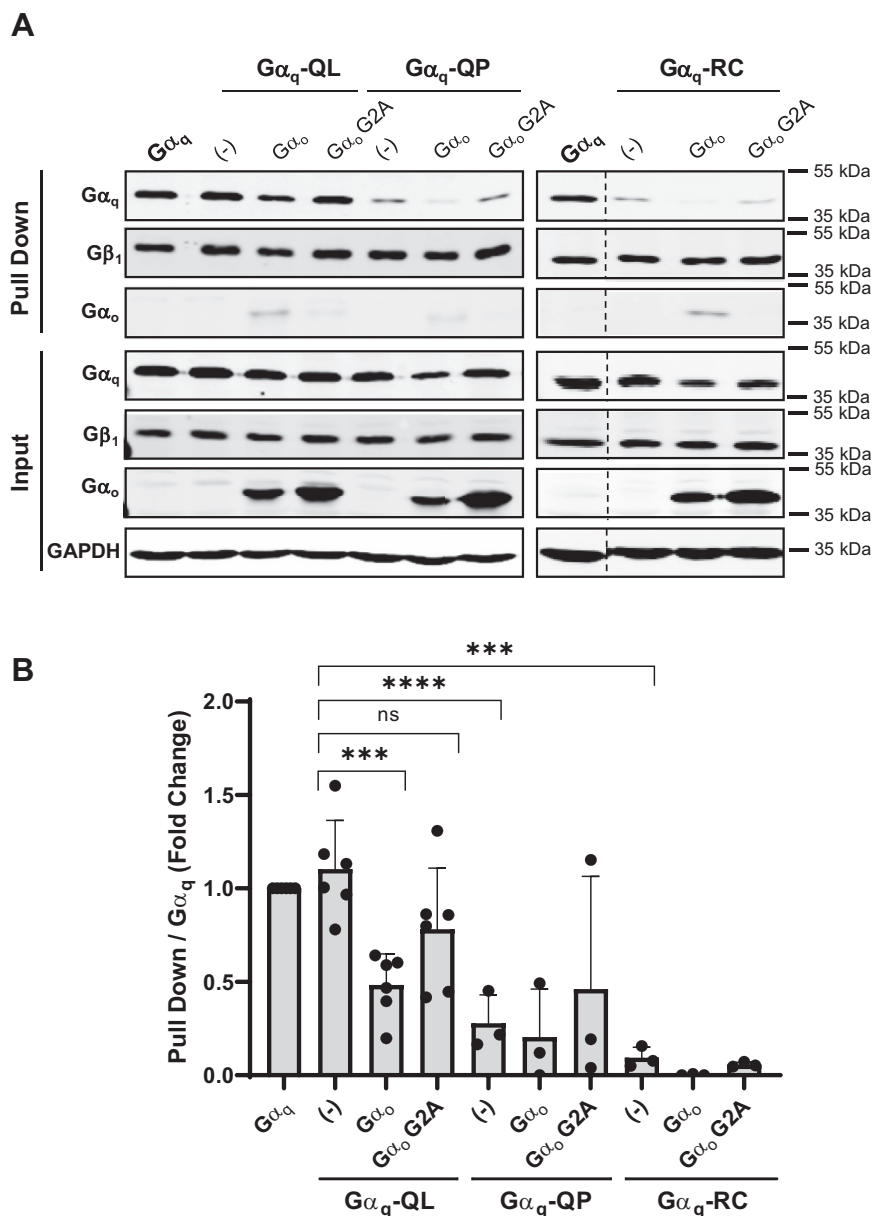


Figure 5. Gα_o expression disrupts Gβγ binding to constitutively active Ga_q mutants. A and B, HEK 293 6x-His-β₁γ₂ stable cells were transfected with WT Ga_q, Ga_q-QL, Ga_q-QP, or Ga_q-RC, along with 300 ng of Gα_o or Gα_o G2A. The cells were lysed, and an Ni-NTA pull-down assay was performed. A, pull down and input lysates were immunoblotted using antibodies for the proteins indicated. B, the Ga_q pull down signal intensities were quantified and normalized to WT Ga_q pull-down signal intensity. Results are shown as mean ± SD. Statistical significance is indicated (n = 3; n = 6 for WT Ga_q, Ga_q-QL, and Ga_q-QL plus Gα_o or Gα_o G2A, ***p < 0.005; ****p < 0.0001, two-way ANOVA, Sidák's multiple comparison's test).

endogenous Gβγ by expression of Gα_o—to show that inhibiting interaction with Gβγ can drastically reduce CA Ga_q-stimulated signaling to both the MAPK and YAP/TAZ pathways. Moreover, signaling by CA Ga_q-Q209P, as well as CA Ga_q-R183C, was much more effectively prevented by Gβγ binding disruption than signaling by CA Ga_q-Q209L. Lastly, we extended the analysis to UM cell lines containing either the oncogenic driver mutant Ga_q-Q209L or Ga_q-Q209P and showed that depletion of Gβ_{1/2} strongly inhibited activation of the MAPK pathway in cells with the Ga_q-Q209P mutant but not in cells with the Ga_q-Q209L. Our results suggest that disrupting the interaction between Gβγ

and CA Ga_q may be a novel approach for inhibiting aberrant Ga_{q/11} signaling.

Although the importance of Gβγ for localization and GPCR-dependent activation of WT, GDP-bound Gα subunits is clearly established, the idea that activated, GTP-bound Gα subunits also require Gβγ to carry out their cellular functions remains poorly defined. Classically, it is generally considered that upon GPCR stimulation, GTP is exchanged for GDP on the Gα subunit, and Gβγ dissociates from Gα. Therefore, if the Gα subunit is “locked” in a GTP-bound state, as would be the case for the GTPase-deficient CA Ga_q mutants studied herein, it would be expected that CA Ga_q mutants would not retain

Gβγ binding is required for mutant Gα_q signaling

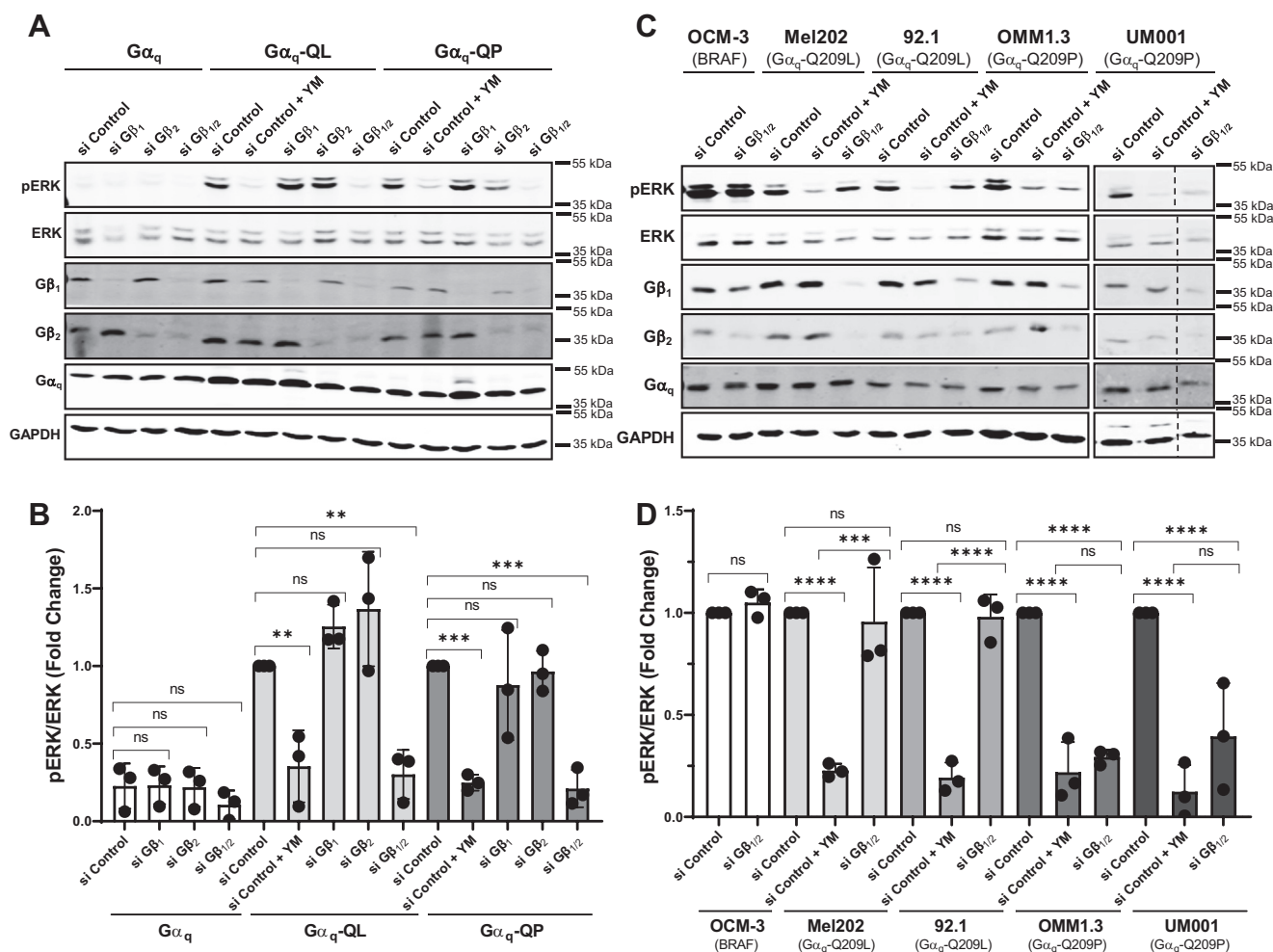


Figure 6. Knockdown of Gβ_{1/2} inhibits oncogenic MAPK signaling in uveal melanoma cells with Gα_q-Q209P mutation. A and B, HEK 293 Gα_q/11 KO cells were transfected with control, Gβ₁, Gβ₂, or Gβ_{1/2} siRNA. After 24 h, cells were transfected with WT Gα_q, Gα_q-QL, or Gα_q-QP. YM indicates treatment with 1 μM YM for 16 h. A, cell lysates were prepared and immunoblotted for pERK, ERK, Gβ₁, Gβ₂, Gα_q, and GAPDH. B, pERK/ERK signal intensities were quantified. Results are shown as mean ± SD. Graph indicates pERK/ERK signal intensities normalized to Gα_q-QL or Gα_q-QP with control siRNA. Statistical significance is indicated (n = 3; **p < 0.01; ***p < 0.005; two-way ANOVA, Tukey's multiple comparison's test). C and D, OCM-3, Mel202, 92.1, OMM1.3, or UM001 cells were transfected with control or Gβ_{1/2} siRNA. YM indicates treatment with 1 μM YM for 16 h. C, cell lysates were prepared and immunoblotted for pERK, ERK, Gβ₁, Gβ₂, Gα_q, and GAPDH. D, pERK/ERK signal intensities were quantified. Results are shown as mean ± SD. Graph indicates pERK/ERK signal intensities normalized to each cell line with control siRNA. Statistical significance is indicated (n = 3; ***p < 0.005; ****p < 0.0001, two-way ANOVA, Tukey's multiple comparison's test). MAPK, mitogen-activated protein kinase; pERK, phospho-ERK.

binding to Gβγ. However, several studies have challenged the classical heterotrimer dissociation model, indicating that at least some Gα subunits maintain association with Gβγ when they are in the active, GTP-bound state due to the presence of a GTPase-inhibiting mutation or in response to GPCR activation (46, 47). The studies presented here using Gβγ pull-down assays (Figs. 2 and 4), along with previous work in our lab and others (35, 36), support the idea that the CA mutant Gα_q-QL retains binding to Gβγ, similar to that of WT Gα_q. Our data also indicate that CA Gα_q-QP and Gα_q-RC can bind Gβγ, although to a much lesser extent than Gα_q-QL. Gβγ pull-down assays show a low level of Gα_q-QP and Gα_q-RC associated with Gβγ, but this pull-down of Gα_q-QP and Gα_q-RC is decreased by the introduction of the I25A mutation or expression of Gβγ-sequestering Gα_o (Figs. 2 and 4). Support for the binding of Gβγ to Gα_q-QP and Gα_q-RC is provided further by our data showing an almost complete loss of

signaling by Gα_q-QP and Gα_q-RC when they contain the I25A mutation or when Gα_o is expressed (Figs. 1, 3 and 4). Importantly, the interaction of CA Gα with Gβγ is not unique to Gα_q. Our previous work showed that CA Gα_s mutants, such as Gα_s-QL and Gα_s-RC, also retain binding to Gβγ (35). More recent work in the field indicates that, along with Gα_q-QL, Gα₁₃-QL also maintains a robust binding association with Gβγ; however, Gα_i-QL does not associate with Gβγ, highlighting an intriguing specificity (36).

A structural view of how CA Gα_q mutants interact with Gβγ and a clear understanding of how Gβγ regulates constitutive signaling by CA Gα_q remain elusive. Crystal structures indicate that the inactive, GDP-bound Gα subunit has two main points of contact with Gβγ: 1) a central switch region, which undergoes a conformational change upon GTP binding and 2) an N-terminal α helical domain (32–34). GTP binding-dependent conformational changes in the Gα switch regions

result in a decreased affinity for Gβγ; however, this appears not to be sufficient for complete disruption of Gα and Gβγ association in some cases. Thus, the Gα N-terminus may play an essential role in maintaining association with Gβγ when Gα is placed in an active conformation by GPCR activation or through the presence of a GTPase-inhibiting mutation. Previous work showing that the N-terminus is essential for Gα interaction with Gβγ and that discrete mutations in the N-termini of several Gα, including Gα_q and Gα_s, are sufficient to disrupt interaction with Gβγ support this model (27, 48–52). Furthermore, a recent study comparing the ability of Gα_q-QL and Gα₁₃-QL to associate with Gβγ with the inability of Gα_i-QL to associate with Gβγ showed that a Gα_{i/13}-QL chimera, in which the N-terminal helix of Gα₁₃-QL is replaced with the N-terminal helix of Gα_i-QL, failed to interact with Gβγ (36). Thus, a clamshell model has been put forth in which GTP-bound Gα and Gβγ “open up” but remain associated through the N-terminus of Gα (46, 47). Nonetheless, this model does not fully explain why Gα_q-QP and Gα_q-RC weakly associate with Gβγ in pull-down assays since Gα_q-QL, Gα_q-QP, and Gα_q-RC have identical N-termini. Intriguingly, in G protein heterotrimer crystal structures (32, 33), Q209 in Gα_q and the corresponding glutamine in Gα_i make contact with Gβ, raising the possibility that the leucine at this position in Q209L promotes interaction with Gβ, either directly or indirectly by effecting a conformational change in Gβ-interacting switch regions. Clearly, future work is needed to understand how activated Gα, such as Gα_q-QL, retain association with Gβγ. The second question of why certain activated Gα need to interact with Gβγ is likewise not well-understood. Association with Gβγ is critical for palmitoylation and membrane localization of Gα_q, and it is known that Gα_q cannot signal when it is not palmitoylated and not membrane-localized (27). A complete lack of signaling by Gα_q-QL-C9,10S, in which the two sites of palmitoylation are mutated, reinforces the requirement for palmitoylation for Gα_q signaling (Fig. 1, A and E). Thus, one reason why CA Gα_q mutants in this study showed decreased or loss of signaling to the MAPK and YAP pathways when interaction with Gβγ is disrupted is a failure to be efficiently palmitoylated and membrane-bound. Indeed, Gα_q-I25A-QL retains stronger plasma membrane localization than Gα_q-I25A-QP and Gα_q-I25A-RC (Fig. S1). Additional roles likely exist for the continued association of CA Gα_q with Gβγ. Notably, our previous work showed that Gα_q-I25A-RC failed to stimulate IP production, consistent with the lack of MAPK and YAP pathway activation observed here, and the introduction of a site for N-terminal myristoylation into Gα_q-I25A-RC to recover palmitoylation and membrane binding failed to recover IP signaling, demonstrating that enhanced membrane localization is not sufficient to overcome the disruption of association with Gβγ (35). Continued association of CA Gα_q with Gβγ may allow both components to simultaneously activate an effector, such as PLC-β; such dual activation of a single effector may be required for efficient signaling in specific contexts. In addition, a recent study showing a strong association of Gα_q-QL and Gα₁₃-QL with Gβγ provided evidence for a model in which retained association with Gβγ prevents Gβγ-

mediated P-REX1-Rac1 signaling while still allowing Gα_q-QL and Gα₁₃-QL to interact with their effectors (36). Moreover, we cannot rule out a role for GPCR stimulation in signaling by the Gα_q mutants and thus a potential role for Gβγ in facilitating GPCR coupling. There are likely to be multiple functional consequences of maintained association of CA Gα_q with Gβγ, and our work here provides a strong demonstration of the importance of retaining interaction with Gβγ for the activation of oncogenic signaling pathways by the Gα_q-QL, Gα_q-QP, and Gα_q-RC mutants that are drivers of UM.

The most novel and striking finding in our studies was that the CA Gα_q-QP and Gα_q-RC mutants are dramatically more sensitive to Gβγ binding disruption than Gα_q-QL. This difference was demonstrated with the introduction of the I25A mutation, expression of Gα_o, and siRNA depletion of Gβ_{1/2}. In all signaling assays tested, the introduction of I25A into Gα_q-QL to generate Gα_q-I25A-QL only partially reduced signaling compared to Gα_q-QL (Fig. 1). On the other hand, Gα_q-I25A-QP and Gα_q-I25A-RC were completely deficient in signaling as measured by TEAD- and SRE-luciferase reporter assays and as detected by YAP localization (Fig. 1, A, B and E), although only partial loss of signaling was observed in when measuring pERK (Fig. 1, C and D). Expression of the increasing amounts of Gα_o to sequester Gβγ provided a powerful tool to demonstrate titratable differences in sensitivity to disruption of Gβγ binding to the CA Gα_q mutants (Figs. 3 and 4). In the TEAD-luciferase assay, transfection with 200 ng of Gα_o expression plasmid resulted in 63% inhibition of Gα_q-QL, but transfection with 100 ng of Gα_o plasmid reduced the signaling of Gα_q-QP and Gα_q-RC by 83% and 84%, respectively (Fig. 3A). Using the SRE-luciferase assay, transfection with 50 ng of Gα_o expression plasmid was sufficient to completely abolish signaling of Gα_q-QP and Gα_q-RC, while transfection with 250 ng of Gα_o plasmid was required to observe a similar almost-complete inhibition of Gα_q-QL signaling (Fig. 4C). Likewise, transfection with 50 or 100 ng of Gα_o plasmid failed to inhibit Gα_q-QL-stimulated pERK levels, but transfection with 50 or 100 ng of Gα_o plasmid provided significant inhibition of Gα_q-QP- and Gα_q-RC-stimulated pERK (Fig. 4, A and B). Gβγ pull-down experiments showed the interaction of Gα_q-QL with Gβγ, similar to the levels of WT Gα_q interaction with Gβγ, and, importantly, the I25A mutation and expression of Gα_o only partially disrupted the interaction (Figs. 2 and 5); these results thus provided a mechanistic interpretation for the inability to fully inhibit Gα_q-QL signaling when Gβγ binding is disrupted. The much lower levels of association with Gβγ of Gα_q-QP and Gα_q-RC, compared to Gα_q-QL, can explain the clear differences in sensitivity to the inhibition of signaling upon disruption of Gβγ binding. Gα_q-QL has a stronger association with Gβγ, which ultimately promotes resistance to the disruption of aberrant cell signaling.

The results presented here are the first to show that signaling by Gα_q-QL *versus* Gα_q-QP can be differentially disrupted. They both contain a single amino acid substitution at Q209, yet exhibit dramatic differences in the ability of their signaling to be inhibited by disruption of the interaction with Gβγ (Figs. 1, 3 and 4). Interestingly, a recent report compared

Gβγ binding is required for mutant Gα_q signaling

Gα_q-QL and Gα_q-QP and found no difference in their signaling ability (40). We confirmed here using multiple signaling assays that Gα_q-QL and Gα_q-QP constitutively activated signaling pathways to a similar degree upon similar protein expression levels (Figs. 1, 3 and 4). However, Maziarz, *et al.* (40) showed that Gα_q-QP compared to Gα_q-QL displayed much lower levels of association with effectors and RGS proteins. It was also observed that whereas Gα_q-QL showed the expected protein fragment in a trypsin protection assay, Gα_q-QP did not, leading to the conclusion that Gα_q-QP exists in a different active conformation compared to Gα_q-QL (40). It seems likely that substitution of Q209 with proline changes the conformational dynamics compared to Gα_q-QL, consistent with differing levels of binding to Gβγ (Figs. 2 and 5) and the consequent differences in the inhibition of signaling that we show here (Figs. 1, 3 and 4).

To further validate the differences in inhibition of Gα_q-QL *versus* Gα_q-QP, we used UM cells containing a Q209L or Q209P mutation in endogenous Gα_q. We used siRNA to deplete endogenous Gβ₁ and Gβ₂ and analyzed constitutively activated levels of pERK (Fig. 6). Depletion of Gβ_{1/2} profoundly inhibited pERK activation in two cell lines, OMM1.3 and UM001, harboring Gα_q-QP, equivalent to inhibition by treatment with the Gα_q inhibitor YM-254890. In contrast, no inhibition of pERK was seen upon Gβ_{1/2} depletion in two UM cell lines, Mel202 and 92.1, containing Gα_q-QL, even though YM-254890 efficiently abolished pERK signaling in those cells. These results provide strong support for the greater sensitivity of Gα_q-QP than Gα_q-QL in terms of inhibition of oncogenic signaling by inhibiting interaction with Gβγ. Interestingly, when Gβ_{1/2} was depleted in HEK 293 Gα_{q/11} KO cells, signaling to pERK was prevented for both overexpressed Gα_q-QL and Gα_q-QP. We suspect that the difference in Gα_q-QL sensitivity in HEK 293 Gα_{q/11} KO cells *versus* UM cells results from the differences in methods when examining the effect of Gβ_{1/2} knockdown on endogenous Gα_q-QL compared to transfected Gα_q-QL. Gβ_{1/2} depletion in HEK 293 Gα_{q/11} KO cells may prevent the subsequently transfected and thus newly synthesized Gα_q-QL from ever localizing to membranes. In contrast, Gβ_{1/2} depletion in UM cells would have to disrupt endogenous Gα_q-QL that is already at membranes and bound to Gβγ. Regardless, our results suggest that disrupting the interaction between Gβγ and CA Gα_q could be a novel therapeutic target in patients with UM, particularly those with the Q209P mutation. Approximately, 90% of patients with UM have mutations at Q209 and 5% have mutations at R183 in Gα_{q/11}, causing constitutive activation of downstream signaling pathways. Mutations in Gα_q and Gα₁₁ are mutually exclusive in UM, with Q209 mutations occurring with similar frequency in Gα_q and Gα₁₁. Interestingly, in a study of 80 patient samples, 34% contained the Gα_q-Q209P mutant, 13% contained the Gα_q-Q209L mutant, and 43% harbored the Gα₁₁-Q209L mutant; no samples with Gα₁₁-Q209P were identified (8). Here, we show that disrupting the association between Gβγ and CA Gα_q disrupts oncogenic signaling involved in UM. Importantly, we suggest that the Gα_q-QP and Gα_q-RC are more sensitive to proliferative cell disruption. The importance of this novel

differential sensitivity between the Gα_q-QL and Gα_q-QP mutations is highlighted by a recent retrospective analysis of 87 metastatic UM patients (53). The authors found no significant change in time from primary tumor diagnosis to liver metastasis between patients with the Gα_{q/11}-QL or Gα_{q/11}-QP mutations; however, patients with the Q209P mutation had significantly higher survival after metastasis than patients with the Q209L mutation. In particular, the median survival rate of patients with the Gα_q-QL mutation was 21.5 months, while the survival rate after metastasis for patients with the Gα_q-QP mutation was 35 months (53). We speculate that the differential binding between the Gα_q-QL and Gα_q-QP mutants with Gβγ and other effectors could potentially have an impact on oncogenicity and survival after metastasis.

Experimental procedures

Plasmids, siRNA, and reagents

HA-tagged WT Gα_q, Gα_q-QL, and Gα_q-RC in pcDNA3 were described previously (35). The Q209P mutation for the Gα_q-QP construct was generated from WT Gα_q *via* site-directed mutagenesis using the primers (Forward: 5' – CGA TGTAGGGGGCCCAAGGTCAGAGAGAAG – 3', Reverse: 5' – CTTCTCTCTGACCTTGGGCCCCCTACATCG – 3'). The Gα_q-I25A, Gα_q-I25A-QL, and Gα_q-I25A-RC constructs were previously described (35). The I25A mutation was generated for Gα_q-I25A-QP from Gα_q-QP (Forward: 5' – GCA GCTGCCGCTCGGCCTCGTCGTTGATCC – 3', Reverse: 5' – GGATCAACGACGAGGCCGAGCGGCAGCTGC – 3'). YFP-tagged Gα_q was provided by Catherine Berlot. Gα_o and Gα_o-G2A plasmids were described previously (44). Lipofectamine 2000 used for Gα_q and Gα_o transient transfections was obtained from Invitrogen (Cat # 11668-019). siRNA targeting Gβ₁ (GGAUAACAUAUUGCUCCAUAU), Gβ₂ (ACUGGGUA CCUGUCGUGUU), and both Gβ₁ and Gβ₂ (Gβ_{1/2}) (ACGACGACUUAACUGCAA) were previously described (54, 55). The ON-TARGET plus nontargeting siRNA (Horizon Discovery, Cat # D-001810-10-20) was used for control siRNA transfections. Lipofectamine RNAiMAX was used for siRNA transfections (Invitrogen, Cat # 13778-150). YM-254890 (YM) was obtained from Wako Chemicals (Cat # 257-00631).

Antibodies

The antibodies for Gα_q (Cat #13927-1-AP) (for immunoblots with HEK 293 Gα_{q/11} KO lysates), GAPDH (Cat # 60004-1-Ig), and Gα_o (Cat # 12635-1-AP) were from Proteintech. The Gα_q (Cat # ab199533) (for immunofluorescence experiments), Gβ₁ (Cat # ab137635), and Gβ₂ (Cat # ab108504) antibodies were obtained from Abcam. The YAP antibody (Cat # sc-101199) was purchased from Santa Cruz. The Gα_q (Cat # 14373S) (for immunoblots with OCM-3, Mel202, 92.1, OMM1.3, and UM001 lysates), ERK (Cat # 4696S), pERK (Cat # 9101S), and Myc-tag (Cat # 2272S) antibodies were obtained from Cell Signaling Technologies. The HA-tag antibody 12CA5 was from Covance. The GRK4-6 antibody (Cat # 05-466) was obtained from Sigma-Aldrich. For immunofluorescence microscopy, the secondary antibodies Alexa Fluor 488

(goat anti-rabbit) (Cat # A-11034), Alexa Fluor 594 (goat anti-mouse) (Cat # A-11032), Alexa Fluor 594 (goat anti-rabbit) (Cat # A-11037), and Alexa Fluor 647 (goat anti-mouse) (Cat # A-32728) were purchased from Invitrogen. The secondary antibodies IRDye 680RD goat anti-rabbit IgG (H + L) (Cat # 92568071) and IRDye 800CW donkey anti-mouse IgG (H + L) (Cat # 92532212) were obtained from LI-COR and were used to visualize protein from all of the immunoblots.

Cell culture and reagents

HEK 293 Gα_{q/11} KO cells were generously provided by Dr Asuka Inoue and were described previously (56). The HEK 293 Gα_{q/11} KO cells were cultured in Dulbecco's modified Eagle's medium (Corning, Cat # 10-017-CV) with 10% fetal bovine serum (FBS) (Gemini, Cat # 900-108) and 1% penicillin/streptomycin (Sigma, Cat # P4333). HEK 293 Gβ₁γ₂ stable cells were described previously (35) and were supplemented with 10% FBS, 1% penicillin/streptomycin, and 0.5 mg/ml of G418 (Invivogen, Cat # ant-gn-5). OCM-3, 92.1, and OMM1.3 cells were provided by Dr Andrew Aplin and have been previously described (19). UM001 cells were also described previously and obtained from Dr Takami Sato (57). The Mel202 cell line was from Dr Bruce Ksander. The OCM-3, 92.1, Mel202, OMM1.3, and UM001 cells were cultured in RPMI 1640 with L-Glutamine and 25 mM Hepes (Corning, Cat # 10-041-CV) supplemented with 10% FBS. All cell culture plates were obtained from Costar, Fisher, or GenClone.

Dual luciferase assay

HEK 293 Gα_{q/11} KO cells were cultured in 12-well plates. Cells were transfected with the corresponding Gα_q and/or Gα_o construct, along with the Renilla luciferase control plasmid and either the 8x-GT1C TEAD luciferase or the SRE luciferase reporter plasmids. The 8x-GT1C TEAD luciferase reporter plasmid was gifted from Stefano Piccolo (Addgene plasmid # 34615). The SRE luciferase reporter plasmid was described previously (58). Lipofectamine 2000 was used for the transfections according to manufacturer's instructions. The media was changed to serum free media, with or without 1 μM YM, 2 h after transfection. After approximately 16 h, the cells were lysed in 1× passive lysis buffer (Promega, Cat # E1941) according to manufacturer's instructions. Cell lysates were plated in triplicate in an opaque white 96-well plate, and luciferase activity was detected using the Dual-Luciferase Reporter Assay System kit and the GloMax Explorer luminometer per manufacturer's instructions. 5x-SDS-PAGE sample buffer with 3.5% β-mercaptoethanol was also added separately to cell lysates and ran on a 10% SDS-PAGE gel and further immunoblotted for Gα_q or Gα_o to measure relative protein expression.

Immunofluorescence microscopy

HEK 293 Gα_{q/11} KO cells were seeded onto coverslips in 6-well plates. For the Gα_q-I25A experiments, pcDNA3, WT Gα_q, or the corresponding CA Gα_q mutants with or without the I25A mutation were transiently transfected into the cells.

For the Gα_o experiments, YFP-tagged Gα_q constructs were cotransfected into cells with 250 ng of Gα_o or Gα_o G2A. Twenty four hours after transfection, the media was changed to serum-free media with or without 1 μM YM. After approximately 16 h, the cells were fixed with 3.7% formaldehyde in PBS for 15 min. The cells were washed 3 times with PBS and blocked for 20 min in 2.5% milk in tris-buffered saline (TBS) with 1% Triton X-100. For the Gα_q-I25A experiments, the cells were incubated with the anti-rabbit Gα_q antibody (Abcam) and the anti-mouse YAP antibody in 2.5% milk/TBS-Triton X-100. For the Gα_o experiments, the cells were incubated with the anti-rabbit Gα_o antibody and the anti-mouse YAP antibody in 2.5% milk/TBS-Triton X-100. The primary antibodies were incubated for 60 min. The cells were washed 5 times with 2.5% milk/TBS-Triton X-100. For the Gα_q-I25A experiments, the cells were incubated with goat anti-rabbit Alexa Fluor 488 and goat anti-mouse Alexa Fluor 594 antibodies in 2.5% milk/TBS-Triton X-100. For the Gα_o experiments, the cells were incubated with goat anti-rabbit Alexa Fluor 594 and goat anti-mouse Alexa Fluor 647 antibodies in 2.5% milk/TBS-Triton X-100. The secondary antibodies were incubated for 30 min. The cells were washed 5 times in TBS/1% Triton X-100. The cells were incubated in DAPI (Thermo Fisher Scientific, Cat#D1306) diluted in warmed PBS for 5 min. The coverslips were rinsed in distilled water and mounted onto glass slides with ProLong Diamond Anti-fade Mountant (Invitrogen, Cat # P36970). The images were acquired using the Olympus IX83 microscope with a 60× oil immersion objective and an ORCA Fusion sCMOS camera (Hamamatsu) controlled by Olympus cellSens software.

Gβ₁γ₂ pull-down assay

The Gβ₁γ₂ pull-down assay was done as previously described (35). Briefly, the HEK 293 Gβ₁γ₂ stable cells were seeded in 6-cm plates. For the experiments with the Gα_q-I25A mutants, pcDNA3, WT Gα_q, or the CA Gα_q mutants with or without the I25A mutation were transiently transfected into the cells. For the Gα_o experiments, the cells were transfected with WT Gα_q or the CA Gα_q mutants. The CA Gα_q mutants were cotransfected with or without 300 ng of Gα_o or Gα_o G2A. After 48 h, the cells were washed with PBS and lysed in 500 μl of lysis buffer C (20 mM Hepes pH 7.5, 100 mM NaCl, 5 mM MgCl₂, 1 mM EDTA, and 0.7% Triton X-100, which were supplemented with the protease inhibitors 2 μg/ml leupeptin, 2 μg/ml aprotinin, and 0.1× cComplete mini protease inhibitor cocktail). The cell lysates were incubated for 1 h on ice and were then centrifuged at 13,000 rpm (10,000g) to pellet the nuclei and insoluble material. Forty microliters of the lysate were reserved separately for the input fraction. The remaining lysate was added to 30 μl of Ni-NTA beads (New England BioLabs, Cat # S1423S) and rotated in an end-over-end rotator for 2 h at 4 °C. The tubes were placed in a magnetic rack, and the remaining supernatant was aspirated. The beads were washed 3 times with lysis buffer C. Fifty microliters of elution buffer (lysis buffer C with 0.25 M Imidazole) were added to elute Gβ₁ and any bound proteins from the Ni-NTA beads.

Gβγ binding is required for mutant Gα_q signaling

Forty microliters of the pull-down eluate were transferred to a new tube. Ten microliters of 5× SDS-PAGE sample buffer with 3.5% β-mercaptoethanol were added to the input fraction and the pull-down fraction. The input and pull-down lysates were separated on a 10% SDS-PAGE gel and protein bound was detected *via* immunoblotting. The blots were probed with the HA-tag and Myc-tag antibody (Cell Signaling Technology). The blots for the Gα_o experiments were also probed with Gα_o and GAPDH. The blots were imaged on LI-COR, and the bands were quantified on the ImageJ software (<https://imagej.nih.gov/ij/>). The pull-down samples in Gα_q-I25A experiments were normalized to its respective input fraction. The pull-down samples in the Gα_o experiments were normalized to WT Gα_q.

pERK/ERK immunoblotting and analysis

Cells were lysed in SDS-PAGE sample buffer. Lysates were run on a 10% SDS-PAGE gel and transferred to a nitrocellulose membrane. The membrane was blocked in 2.5% bovine serum albumin (BSA) (Sigma Aldrich, Cat # A7906-100G) in 1× TBS supplemented with 0.05% Tween 20. The blots were incubated with both pERK (Rabbit, Cell Signaling, Cat # 9101S) and ERK (Mouse, Cell Signaling, Cat # 4696S) antibodies overnight. A duplicate immunoblot was performed and was probed with either Proteintech Gα_q (Rabbit, Cat #13927-1-AP) for the HEK 293 Gα_{q/11} KO cells or Cell Signaling Gα_q (Rabbit, Cat # 14373S) for the UM cells, along with GAPDH (Mouse, Proteintech, Cat # 60004-1-Ig) as a loading control. The ERK and pERK bands were quantified by densitometry using the ImageJ software, and the relative pERK signal was divided by ERK. The quantified signals were normalized to WT Gα_q (Fig. 1D), the individual CA Gα_q mutants (Fig. 4B), or control siRNA between the CA Gα_q mutants (Fig. 6B) or the UM cell lines (Fig. 6D).

Gβ_{1/2} siRNA transfections

Cells were plated in 6-well plates for the HEK 293 Gα_{q/11} KO cells and 12-well plates for the UM cells. For the HEK 293 Gα_{q/11} KO experiments, 30 pmol of control, Gβ₁, Gβ₂, or Gβ_{1/2} siRNA were transfected into cells using Lipofectamine RNAiMax (Invitrogen, Cat # 13778-150), according to manufacturer's instructions. The media was changed after 5 h. After 24 h, the corresponding WT Gα_q, Gα_q-QL, or Gα_q-QP constructs were transfected into the cells using Lipofectamine 2000 (Invitrogen, Cat # 11668-019). The media was changed to serum-free media after 24 h and corresponding cells were treated with 1 μM of YM. The cells were lysed in 1× SDS-PAGE sample buffer with 0.7% β-mercaptoethanol after 16 h. For experiments with the UM cells, 15pmol of control or Gβ_{1/2} siRNA were transfected into cells using Lipofectamine RNAiMax (Invitrogen, Cat # 13778-150). The media was changed after 5 h. After 72 h, the media was changed to serum-free media, and the corresponding cells were treated with 1 μM of YM. The cells were further lysed after approximately 16 h in 1× SDS-PAGE sample buffer with 0.7% β-mercaptoethanol. The lysates were run on 10% SDS-PAGE

gels and were immunoblotted for pERK (Cell Signaling, Cat # 9101S), ERK (Cell Signaling, Cat # 4696S), Gβ₁ (Abcam, Cat # ab137635), Gβ₂ (Abcam, Cat # ab108504), GAPDH (Proteintech, Cat # 60004-1-Ig), and Proteintech Gα_q (Cat #13927-1-AP) for the HEK 293 Gα_{q/11} KO cells or Cell Signaling Gα_q (Cat # 14373S) for the UM cells.

Western blotting

Protein lysates were run on 10% SDS-PAGE gels and transferred to LI-COR nitrocellulose membranes (Cat # nc9680617). The membranes were blocked in either 2.5% BSA or 2.5% milk in 1× TBS/0.05% Tween 20 at room temperature for 60 min. The blots were incubated in corresponding primary antibodies in 2.5% BSA or milk in 1× TBS/0.05% Tween 20 at 4 °C overnight. The blots were washed three times in 1× TBS/0.05% Tween 20 and incubated in LI-COR anti-rabbit (Cat # 92568071) and anti-mouse (Cat # 92532212) secondary antibodies for 60 min at room temperature. The immunoblots were further washed three times in 1× TBS/0.05% Tween 20 and once with PBS. The blots were then imaged on the LI-COR Odyssey imager.

Statistical analysis

GraphPad Prism was used to analyze the data for all of the figures. A two-way ANOVA followed by Šidák's or Tukey's (Fig. 6, B and D) multiple comparison test were used to calculate significance. Error bars in all experiments indicate mean ± SD with significant differences indicated as **p* < 0.05; ***p* < 0.01; ****p* < 0.005; *****p* < 0.0001.

Data availability

All data is contained within the article.

Supporting information—This article contains supporting information.

Acknowledgments—HEK 293 Gα_{q/11} KO cells were generously provided by Dr Asuka Inoue and Tohoku University (Sendai, Japan), and uveal melanoma cells were kindly provided by Drs Takami Sato and Andrew Aplin (Thomas Jefferson University). We thank Dr Jonathan Brody (Thomas Jefferson University) for the use of their Glomax Explore luminometer and Dr Samantha Brown (Thomas Jefferson University) for assistance. We are grateful to Dr Karen Knudsen and the Department of Cancer Biology (Thomas Jefferson University) for sharing their LI-COR Odyssey imager. We thank Morgan Dwyer, Dr Kalpana Rajanala, and Dr Jeff Benovic for critical reading of the article, and Dr Nevin Lambert for helpful discussion and suggestions.

Author contributions—J. L. A. and P. B. W. conceptualization; J. L. A. investigation; J. L. A. data curation; J. L. A. and P. B. W. writing—original draft; J. L. A. and P. B. W. writing—review and editing; P. B. W. supervision; P. B. W. funding acquisition.

Funding and additional information—This work was supported by the Department of Defense grant ME200047, National Institutes of Health (NIH) Grant R01 GM138943, Dr Ralph and Marian Falk Medical Research Trust (P. B. W.), and NIH Grant T32 GM144302

(J. L. A.). The content is solely the responsibility of the authors and does not necessarily represent the official views of the National Institutes of Health.

Conflict of interest—The authors declare that they have no conflicts of interest with the contents of this article.

Abbreviations—The abbreviations used are: BSA, bovine serum albumin; CA, constitutively active; FBS, fetal bovine serum; GPCR, G protein-coupled receptor; IP, inositol phosphate; MAPK, mitogen-activated protein kinase; pERK, phospho-ERK; PLC-β, phospholipase C-β; SRE, serum response element; TBS, tris-buffered saline; TEAD, TEA domain; UM, uveal melanoma; YAP, Yes-associated protein.

References

- Oldham, W. M., and Hamm, H. E. (2008) Heterotrimeric G protein activation by G-protein-coupled receptors. *Nat. Rev. Mol. Cell Biol.* **9**, 60–71
- Wu, D. Q., Lee, C. H., Rhee, S. G., and Simon, M. I. (1992) Activation of phospholipase C by the alpha subunits of the G_q and G₁₁ proteins in transfected Cos-7 cells. *J. Biol. Chem.* **267**, 1811–1817
- Lapadula, D., and Benovic, J. L. (2021) Targeting oncogenic Galphaq/11 in uveal melanoma. *Cancers (Basel)* **13**
- Offermanns, S. (2003) G-proteins as transducers in transmembrane signalling. *Prog. Biophys. Mol. Biol.* **83**, 101–130
- Landis, C. A., Masters, S. B., Spada, A., Pace, A. M., Bourne, H. R., and Vallar, L. (1989) GTPase inhibiting mutations activate the alpha chain of Gs and stimulate adenylyl cyclase in human pituitary tumours. *Nature* **340**, 692–696
- O'Hayre, M., Vazquez-Prado, J., Kufareva, I., Stawiski, E. W., Handel, T. M., Seshagiri, S., et al. (2013) The emerging mutational landscape of G proteins and G-protein-coupled receptors in cancer. *Nat. Rev. Cancer* **13**, 412–424
- Chua, V., Lapadula, D., Randolph, C., Benovic, J. L., Wedegaertner, P. B., and Aplin, A. E. (2017) Dysregulated GPCR signaling and therapeutic options in uveal melanoma. *Mol. Cancer Res.* **15**, 501–506
- Robertson, A. G., Shih, J., Yau, C., Gibb, E. A., Oba, J., Mungall, K. L., et al. (2017) Integrative analysis identifies four molecular and clinical subsets in uveal melanoma. *Cancer Cell* **32**, 204–220.e15
- Van Raamsdonk, C. D., Bezrookove, V., Green, G., Bauer, J., Gaugler, L., O'Brien, J. M., et al. (2009) Frequent somatic mutations of GNAQ in uveal melanoma and blue naevi. *Nature* **457**, 599–602
- Van Raamsdonk, C. D., Griewank, K. G., Crosby, M. B., Garrido, M. C., Vemula, S., Wiesner, T., et al. (2010) Mutations in GNA11 in uveal melanoma. *N. Engl. J. Med.* **363**, 2191–2199
- Singh, A. D., Bergman, L., and Seregard, S. (2005) Uveal melanoma: epidemiologic aspects. *Ophthalmol. Clin. North Am.* **18**, 75–84. viii
- Shields, C. L., Kaliki, S., Livesey, M., Walker, B., Garoon, R., Bucci, M., et al. (2013) Association of ocular and oculodermal melanocytosis with the rate of uveal melanoma metastasis: analysis of 7872 consecutive eyes. *JAMA Ophthalmol.* **131**, 993–1003
- Chen, X., Wu, Q., Depeille, P., Chen, P., Thornton, S., Kalirai, H., et al. (2017) RasGRP3 mediates MAPK pathway activation in GNAQ mutant uveal melanoma. *Cancer Cell* **31**, 685–696.e6
- Feng, X., Arang, N., Rigracciolo, D. C., Lee, J. S., Yeerna, H., Wang, Z., et al. (2019) A platform of synthetic lethal gene interaction networks reveals that the GNAQ uveal melanoma oncogene controls the Hippo pathway through FAK. *Cancer Cell* **35**, 457–472.e5
- Feng, X., Degese, M. S., Iglesias-Bartolome, R., Vaque, J. P., Molinolo, A. A., Rodrigues, M., et al. (2014) Hippo-independent activation of YAP by the GNAQ uveal melanoma oncogene through a trio-regulated rho GTPase signaling circuitry. *Cancer Cell* **25**, 831–845
- Carvajal, R. D., Sosman, J. A., Quevedo, J. F., Milhem, M. M., Joshua, A. M., Kudchadkar, R. R., et al. (2014) Effect of selumetinib vs chemotherapy on progression-free survival in uveal melanoma: a randomized clinical trial. *JAMA* **311**, 2397–2405
- Steeb, T., Wessely, A., Ruzicka, T., Heppt, M. V., and Berking, C. (2018) How to MEK the best of uveal melanoma: a systematic review on the efficacy and safety of MEK inhibitors in metastatic or unresectable uveal melanoma. *Eur. J. Cancer* **103**, 41–51
- Brouwer, N. J., Konstantinou, E. K., Gragoudas, E. S., Marinkovic, M., Luyten, G. P. M., Kim, I. K., et al. (2021) Targeting the YAP/TAZ pathway in uveal and conjunctival melanoma with verteporfin. *Invest Ophthalmol. Vis. Sci.* **62**, 3
- Lapadula, D., Farias, E., Randolph, C. E., Purwin, T. J., McGrath, D., Charpentier, T. H., et al. (2019) Effects of oncogenic Galphaq and Galpha11 inhibition by FR900359 in uveal melanoma. *Mol. Cancer Res.* **17**, 963–973
- Annala, S., Feng, X., Shridhar, N., Eryilmaz, F., Patt, J., Yang, J., et al. (2019) Direct targeting of Galphaq and Galpha11 oncoproteins in cancer cells. *Sci. Signal* **12**, eaau5948
- Onken, M. D., Makepeace, C. M., Kaltenbronn, K. M., Kanai, S. M., Todd, T. D., Wang, S., et al. (2018) Targeting nucleotide exchange to inhibit constitutively active G protein alpha subunits in cancer cells. *Sci. Signal* **11**, eaao6852
- Takasaki, J., Saito, T., Taniguchi, M., Kawasaki, T., Moritani, Y., Hayashi, K., et al. (2004) A novel Galphaq/11-selective inhibitor. *J. Biol. Chem.* **279**, 47438–47445
- Schlegel, J. G., Tahoun, M., Seidinger, A., Voss, J. H., Kuschak, M., Kehraus, S., et al. (2021) Macrocyclic Gq protein inhibitors FR900359 and/or YM-254890-fit for translation? *ACS Pharmacol. Transl. Sci.* **4**, 888–897
- Onken, M. D., Makepeace, C. M., Kaltenbronn, K. M., Choi, J., Hernandez-Aya, L., Weilbaecher, K. N., et al. (2021) Targeting primary and metastatic uveal melanoma with a G protein inhibitor. *J. Biol. Chem.* **296**, 100403
- Hitchman, T. D., Bayshtok, G., Ceraudo, E., Moore, A. R., Lee, C., Jia, R., et al. (2021) Combined inhibition of Galphaq and MEK enhances therapeutic efficacy in uveal melanoma. *Clin. Cancer Res.* **27**, 1476–1490
- Evanko, D. S., Thiagarajan, M. M., Siderovski, D. P., and Wedegaertner, P. B. (2001) Gbeta gamma isoforms selectively rescue plasma membrane localization and palmitoylation of mutant Galphas and Galphaq. *J. Biol. Chem.* **276**, 23945–23953
- Evanko, D. S., Thiagarajan, M. M., and Wedegaertner, P. B. (2000) Interaction with Gbetagamma is required for membrane targeting and palmitoylation of Galpha(s) and Galpha(q). *J. Biol. Chem.* **275**, 1327–1336
- Fishburn, C. S., Pollitt, S. K., and Bourne, H. R. (2000) Localization of a peripheral membrane protein: gbetagamma targets Galpha(Z). *Proc. Natl. Acad. Sci. U. S. A.* **97**, 1085–1090
- Duc, N. M., Kim, H. R., and Chung, K. Y. (2015) Structural mechanism of G protein activation by G protein-coupled receptor. *Eur. J. Pharmacol.* **763**, 214–222
- Michaelson, D., Ahearn, I., Bergo, M., Young, S., and Philips, M. (2002) Membrane trafficking of heterotrimeric G proteins via the endoplasmic reticulum and Golgi. *Mol. Biol. Cell* **13**, 3294–3302
- Takida, S., and Wedegaertner, P. B. (2003) Heterotrimer formation, together with isoprenylation, is required for plasma membrane targeting of Gbetagamma. *J. Biol. Chem.* **278**, 17284–17290
- Lambright, D. G., Sondek, J., Bohm, A., Skiba, N. P., Hamm, H. E., and Sigler, P. B. (1996) The 2.0 Å crystal structure of a heterotrimeric G protein. *Nature* **379**, 311–319
- Nishimura, A., Kitano, K., Takasaki, J., Taniguchi, M., Mizuno, N., Tago, K., et al. (2010) Structural basis for the specific inhibition of heterotrimeric Gq protein by a small molecule. *Proc. Natl. Acad. Sci. U. S. A.* **107**, 13666–13671
- Wall, M. A., Coleman, D. E., Lee, E., Iniguez-Lluhi, J. A., Posner, B. A., Gilman, A. G., et al. (1995) The structure of the G protein heterotrimer Gi alpha 1 beta 1 gamma 2. *Cell* **83**, 1047–1058
- Evanko, D. S., Thiagarajan, M. M., Takida, S., and Wedegaertner, P. B. (2005) Loss of association between activated Galpha q and Gbetagamma

- disrupts receptor-dependent and receptor-independent signaling. *Cell Signal* **17**, 1218–1228
36. Cervantes-Villagrana, R. D., Adame-Garcia, S. R., Garcia-Jimenez, I., Color-Aparicio, V. M., Beltran-Navarro, Y. M., Konig, G. M., *et al.* (2019) Gbetagamma signaling to the chemotactic effector P-REX1 and mammalian cell migration is directly regulated by Galphaq and Galpha13 proteins. *J. Biol. Chem.* **294**, 531–546
37. Wedegaertner, P. B., Chu, D. H., Wilson, P. T., Levis, M. J., and Bourne, H. R. (1993) Palmitoylation is required for signaling functions and membrane attachment of Gq alpha and Gs alpha. *J. Biol. Chem.* **268**, 25001–25008
38. Liu-Chittenden, Y., Huang, B., Shim, J. S., Chen, Q., Lee, S. J., Anders, R. A., *et al.* (2012) Genetic and pharmacological disruption of the TEAD-YAP complex suppresses the oncogenic activity of YAP. *Genes Dev.* **26**, 1300–1305
39. Ramos, A., and Camargo, F. D. (2012) The Hippo signaling pathway and stem cell biology. *Trends Cell Biol.* **22**, 339–346
40. Maziarz, M., Leyme, A., Marivin, A., Luebbbers, A., Patel, P. P., Chen, Z., *et al.* (2018) Atypical activation of the G protein Galphaq by the oncogenic mutation Q209P. *J. Biol. Chem.* **293**, 19586–19599
41. Faure, M., Voyno-Yasenetskaya, T. A., and Bourne, H. R. (1994) cAMP and beta gamma subunits of heterotrimeric G proteins stimulate the mitogen-activated protein kinase pathway in COS-7 cells. *J. Biol. Chem.* **269**, 7851–7854
42. Selbie, L. A., King, N. V., Dickenson, J. M., and Hill, S. J. (1997) Role of G-protein beta gamma subunits in the augmentation of P2Y2 (P2U)receptor-stimulated responses by neuropeptide Y Y1 Gi/o-coupled receptors. *Biochem. J.* **328**, 153–158
43. Stephens, G. J., and Mochida, S. (2005) G protein {beta}{gamma} subunits mediate presynaptic inhibition of transmitter release from rat superior cervical ganglion neurones in culture. *J. Physiol.* **563**, 765–776
44. Takida, S., Fischer, C. C., and Wedegaertner, P. B. (2005) Palmitoylation and plasma membrane targeting of RGS7 are promoted by alpha o. *Mol. Pharmacol.* **67**, 132–139
45. Griewank, K. G., Yu, X., Khalili, J., Sozen, M. M., Stempke-Hale, K., Bernatchez, C., *et al.* (2012) Genetic and molecular characterization of uveal melanoma cell lines. *Pigment Cell Melanoma Res.* **25**, 182–187
46. Chung, Y. K., and Wong, Y. H. (2021) Re-examining the 'Dissociation Model' of G protein activation from the perspective of Gbetagamma signaling. *FEBS J.* **288**, 2490–2501
47. Lambert, N. A. (2008) Dissociation of heterotrimeric g proteins in cells. *Sci. Signal* **1**, re5
48. Mazzoni, M. R., Malinski, J. A., and Hamm, H. E. (1991) Structural analysis of rod GTP-binding protein, Gt. Limited proteolytic digestion pattern of Gt with four proteases defines monoclonal antibody epitope. *J. Biol. Chem.* **266**, 14072–14081
49. Mazzoni, M. R., and Hamm, H. E. (1989) Effect of monoclonal antibody binding on alpha-beta gamma subunit interactions in the rod outer segment G protein, Gt. *Biochemistry* **28**, 9873–9880
50. Fung, B. K., and Nash, C. R. (1983) Characterization of transducin from bovine retinal rod outer segments. II. Evidence for distinct binding sites and conformational changes revealed by limited proteolysis with trypsin. *J. Biol. Chem.* **258**, 10503–10510
51. Denker, B. M., Neer, E. J., and Schmidt, C. J. (1992) Mutagenesis of the amino terminus of the alpha subunit of the G protein Go. *In vitro* characterization of alpha o beta gamma interactions. *J. Biol. Chem.* **267**, 6272–6277
52. Graf, R., Mattera, R., Codina, J., Estes, M. K., and Birnbaumer, L. (1992) A truncated recombinant alpha subunit of Gi3 with a reduced affinity for beta gamma dimers and altered guanosine 5'-3-O-(thio)triphosphate binding. *J. Biol. Chem.* **267**, 24307–24314
53. Terai, M., Shimada, A., Chervoneva, I., Hulse, L., Danielson, M., Swensen, J., *et al.* (2021) Prognostic values of G-protein mutations in metastatic uveal melanoma. *Cancers (Basel)* **13**, 5749
54. Irannejad, R., and Wedegaertner, P. B. (2010) Regulation of constitutive cargo transport from the trans-Golgi network to plasma membrane by Golgi-localized G protein betagamma subunits. *J. Biol. Chem.* **285**, 32393–32404
55. Rajanala, K., Klayman, L. M., and Wedegaertner, P. B. (2021) Gbetagamma regulates mitotic Golgi fragmentation and G2/M cell cycle progression. *Mol. Biol. Cell* **32**, br2
56. Schrage, R., Schmitz, A. L., Gaffal, E., Annala, S., Kehraus, S., Wenzel, D., *et al.* (2015) The experimental power of FR900359 to study Gq-regulated biological processes. *Nat. Commun.* **6**, 10156
57. Ozaki, S., Vuyyuru, R., Kageyama, K., Terai, M., Ohara, M., Cheng, H., *et al.* (2016) Establishment and characterization of orthotopic mouse models for human uveal melanoma hepatic colonization. *Am. J. Pathol.* **186**, 43–56
58. Helms, M. C., Grabocka, E., Martz, M. K., Fischer, C. C., Suzuki, N., and Wedegaertner, P. B. (2016) Mitotic-dependent phosphorylation of leukemia-associated RhoGEF (LARG) by Cdk1. *Cell Signal* **28**, 43–52